

DIPLOMARBEIT

INTRAZELLULÄRE FÄRBUNGEN UND 3D
STRUKTURANALYSE VON OLFAKTORISCHEN
PROJEKTIONSNEURONEN IM BIENENGEHIRN



VORGELEGT VON:

DANIEL MÜNCH

ANGEFERTIGT AM INSTITUT FÜR BIOLOGIE
AG NEUROBIOLOGIE
FACHBEREICH BIOLOGIE, CHEMIE, PHARMAZIE DER FREIEN UNIVERSITÄT BERLIN

DEZEMBER 2007
BERLIN

Eidesstattliche Versicherung

Hiermit versichere ich an Eides statt, dass ich die vorliegende Diplomarbeit ohne fremde Hilfe angefertigt und dafür keine anderen außer den angegebenen Quellen und Hilfsmitteln verwendet habe.

Berlin, den 11. Dezember 2007

(Daniel Münch)

Erstgutachter: Prof. Dr. Dr. h.c. Randolph Menzel
Zweitgutachter: PD Dr. Bernd Grünwald

Contents

| | |
|---|------------|
| Eidesstattliche Versicherung | ii |
| Contents | iii |
| 1 Summary | 1 |
| 2 Introduction | 2 |
| 2.1 The olfactory pathway | 3 |
| 2.2 The mushroom bodies | 6 |
| 2.3 The honeybee as a model | 8 |
| 2.4 Aim of this study | 9 |
| 3 Material and Methods | 10 |
| 3.1 Animals | 10 |
| 3.2 Preparation | 10 |
| 3.3 Intracellular staining | 11 |
| 3.4 Confocal microscopy | 12 |
| 3.5 Reconstruction | 13 |
| 3.6 Data evaluation | 13 |
| 3.6.1 Image & data processing | 13 |
| 3.6.2 SkeletonTree | 14 |
| 3.6.3 Lip zones | 14 |
| 3.6.4 Bouton distribution | 15 |
| 3.7 Used solutions | 15 |
| 4 Results | 16 |
| 4.1 Innervation of the antennal lobe | 17 |
| 4.1.1 Glomeruli | 19 |
| 4.1.2 Soma location | 19 |
| 4.1.3 Arborizations | 21 |
| 4.2 Innervation of the mushroom body | 22 |
| 4.2.1 Branching pattern | 22 |
| 4.2.2 Boutons | 22 |
| 4.2.3 Bouton distribution within the lip neuropil | 27 |
| 4.3 Protocerebral projections outside the MBs | 34 |
| 4.3.1 Lateral protocerebral lobe | 34 |

| | |
|--|-----------|
| 5 Discussion | 39 |
| 5.1 PNs innervating T4 cluster glomeruli | 39 |
| 5.2 Projections of m- and l-ACT PNs | 43 |
| 5.3 Outlook | 47 |
| Bibliography | v |
| Danksagung | x |

1 Summary

In the brain of the honeybee *Apis mellifera* olfactory information from the antennal lobes, the first olfactory centers, is conveyed to the mushroom bodies and the lateral protocerebral lobe via projection neurons (PNs) running in two separate antenno-cerebral tracts (ACTs). The mushroom bodies are higher order brain centers that get input of various sensory modalities and are involved in learning and memory.

As projection neurons of both tracts were shown to differ in their response patterns to olfactory stimuli and and their innervation of the mushroom bodies and the lateral horn, this study analyzed the anatomy of single stained ACT neurons with conventional and 3D techniques, based on newly designed tools. With this analysis the further subdivision of the mushroom body's lips into zones as found earlier could be approved, but a clear innervation of parts solely by either tract could not be observed on a single cell level. Segregation of olfactory input to defined zones of the lateral horn could be approved. Domain-like innervation patterns within the lip neuropil could be shown on single ACT reconstructions and ACTs of both tracts could be demonstrated to express *en passant* blebs in a distal collar zone. Three projection neurons which run along the m-ACT and send their dendrites to glomeruli of the T4 cluster were found to exhibit different morphologies than m-ACT PNs originating from other glomeruli.

2 Introduction

In order to perceive stimuli cues from their environment, to communicate with other individuals and to find and evaluate the quality of food sources, animals use various senses. The evolutionary oldest and broadest distributed through the whole tree of life are those sensory systems specific for detecting chemical substances of all kinds. Any protozoan and nearly every cell of a metazoan body has specific receptors either attached to its membrane or inside its lumen. The use of chemical senses is crucial for the survival of animals in many different situations, may it be the bitter or sour taste of bad milk that prevents us from drinking it, or the smell of a predator that leads to the preys flight. Of these two chemosensory systems, the gustatory and the olfactory, the last one is by far the complexest. By taste we can discriminate the number of five basic qualities (sweet, sour, salty, bitter and umami) but we are able to sense thousands of different odors may they consist out of a single component or be a complex mixture.

How much any sense contributes to the complete picture an animal is acquiring of its environment depends on the surrounding itself and the specialization every species has developed within its ecological niche. For honeybees olfactory cues are clearly one of the most important to perceive. As a social insect with division of labor, the life of the colony critically depends on communication from which at least one part

is achieved by the use of pheromones the queen is emitting to prevent workers from building new queen combs and raising contenders. Another communicative task which depends on olfaction is a part of the waggle dance (von Frisch, 1967), when foragers pass along the position and quality of valuable food sources, they give away samples by trophallaxis and by this also transmit the odor of the substance of interest. These newly recruited foragers already learn the odor of the new food source during this act of trophallaxis (Farina et al., 2007; Arenas et al., 2007).

This ability to learn odors and associate them with food sources or a special context can not only be observed in free living bees but also under lab conditions with free flying or harnessed bees (Takeda, 1967). One approach to study olfactory learning in honeybees is to make use of the proboscis extension response (PER), in which a bee is fixed into a small plastic tube with only its antennae and mouth parts left freely movable (Kuwabara, 1957; Takeda, 1967). When the antennae is touched with a sucrose solution the bee will extend its proboscis (PER). If an odor, provided via an air stream onto the antennae, is paired with this sucrose stimulation, the animal will extend its proboscis to the odor stimulation alone after only one trial. The odor which serves as a conditioned stimulus (CS) is learned to be rewarded with sucrose, the unconditioned stimulus (US) (Bittermann et al., 1983).

2.1 The olfactory pathway

The basic morphological structures used for olfactory processing within the honeybee brain are well known and described in various publications, an schematic overview can be seen in figure 1. The main parts for odor detection are the bees antennae, to be more precise the most distal part, the flagellum. These flagella are peppered

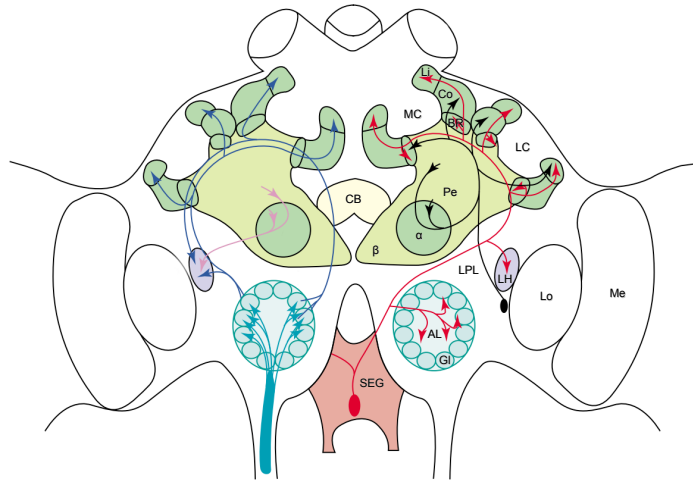


Figure 1: A schematic overview over the brain of *Apis mellifera* with some neurons constituting the olfactory pathway. Olfactory receptor neurons (light blue arrows) enter the approximately 156 glomeruli (Gl) of the first olfactory neuropils, the antennal lobes (AL, light blue). Information is conveyed via a medial and a lateral antenniferous tract (ACT, dark blue arrows) towards higher order neuropils, the mushroom bodies (MB, green) and the lateral horn (LH, violet). SEG, sub esophageal ganglion; CB, central body; MC, medial calyx; LC, lateral calyx; Li, lip; Co, collar; BR, basal ring; Pe, pedunculus; α , alpha lobe; β , beta lobe; LPL, lateral protocerebral lobe; red arrows, VUM_{mx1}; black arrows, inhibitory feedback neurons; violet arrows, MB output neurons. (modified from Menzel and Giurfa 2001).

with sensilla in which approximately 60,000 olfactory receptor neurons (ORNs) per antenna reside (Esslen and Kaissling, 1976; Kelber et al., 2006). The ORNs are sending their axons via four antennal tracts, T1-T4 (Suzuki, 1975), into the antennal lobes, the first integrative neuropil along the olfactory pathway. The antennal lobes are build out of 156 to 166 spherical structures, the glomeruli (Arnold et al., 1985; Flanagan and Mercer, 1989) which are interconnected by approximately 4,000 local interneurons of which around 5 % show immunoreactivity to GABA and hence might be inhibitory (Bicker, 1999). The glomeruli can be assigned to four clusters each getting input from a single antennal tract and hereby also named T1-T4. The antennal lobe is responding to olfactory stimulation in an odor specific code of glomerular activity (Galizia et al., 1999b; Sachse and Galizia, 2003) which emphasizes the role as an integrative unit for the ORNs input. This scheme of connectivity and the glomerular structure of the

antennal lobes is analogue to the olfactory bulb, the first order olfactory neuropil in the mammalian olfactory pathway (Hildebrand and Shepherd, 1997).

The output of the antennal lobes is conveyed to higher brain areas via five tracts of olfactory projection neurons (PNs), the medial antennocerebral tract (m-ACT), the lateral antennocerebral tract (l-ACT) and three mediolateral tracts (ml-ACT). Neurons running in the m- and l-ACT are always sending their dendrites to only one glomerulus whereas ml-ACT neurons show multiglomerular innervation patterns (Abel et al., 2001; Kirschner et al., 2006). L-ACT PNs are innervating glomeruli of the T1 cluster exclusively, m-ACT PNs get their input from the three remaining clusters T2-T4

L-ACT neurons are leaving the antennal lobe dorsally and run through the lateral protocerebrum towards the ipsilateral mushroom body (MB) where they branch off in several collaterals with their endings located in the lip neuropil (Bicker et al., 1993; Abel et al., 2001; Kirschner et al., 2006). On their way towards the MBs l-ACT neurons send a collateral towards the lateral horn (LH). M-ACT neurons innervate similar regions but run the other way round, projecting to the MBs first, bypassing the alpha lobe medial between central body (CB) and MB, and then running towards the lateral protocerebral lobe (LPL). Approximately 800 PNs are running in both tracts (Rybäk, 1994).

Both m- and l-ACT neurons show bouton-like structures on their terminals in the lip and the LH and *en passant*-like blebs within the same regions and additional in the basal ring (BR). These boutons represent presynaptic swellings and therefore indicate putative output regions (Schürmann, 1974; Mobbs, 1982; Ganeshina and Menzel, 2001). The three tracts of the ml-ACTs on the other hand do not project to the MBs but innervate regions within the LPL and the ring neuropil around the

alpha lobes exclusively (Kirschner et al., 2006).

2.2 The mushroom bodies

The mushroom bodies are two very prominent, bilateral symmetric structures belonging to the protocerebrum of an insects brain (Kenyon, 1896). In social hymenopteran insects like ants, wasps an bees, the MBs are especially big in relation to the whole brain which early led to the assumption of their involvement in complex social behavior an learning and memory (Howse, 1974). Different studies were able to show multimodal sensory input to the MBs and that they play a role in memory formation could be verified by experiments where focal cooling was applied to these structures at different time points after single trial conditioning (Erber et al., 1980).

In the honeybee the MBs are build out of two main neuropils, the cup shaped calyces. A medial and a lateral one, which are morphological connected via the Y-shaped pedunculus that branches off two lobes within the central protocerebral lobe. One ventral or alpha lobe that is orientated anterior, with respect to the body axis, and one medial or beta lobe heading towards the brains midline (Fig. 1).

While the calyces represent the main input region of the MBs, getting input from various sensory brain regions, the lobes in contrast show mainly output features with the alpha lobe for example connected to around 400 extrinsic neurons originating from 7 soma clusters and showing a variety of projections within or outside the MBs (Rybäk and Menzel, 1993). The calyces can further be divided into three concentric compartments (Fig. 1) based on their morphological structure and the input they receive. Those compartments are, from the ventral to the dorsal part of the calyx, the

basal ring, the collar and the lip. The lip mainly receives olfactory input from the ALs, the collar receives direct optical input from both, medulla and lobula, and the basal ring receives both, olfactory and visual input (Gronenberg, 2001; Ehmer and Gronenberg, 2002).

The size and shape of the MBs varies across taxa and also exhibits the compartment's specialization, a basal ring for example can not be distinguished in most ants and a collar can not be found in blind ants (Gronenberg, 2001). However, different staining techniques and innervation pattern of either MB intrinsic or extrinsic cells reveal further possible subdivisions of the three calycal compartments (Gronenberg, 2001; Strausfeld, 2002; Kirschner et al., 2006).

Differences in optical density and texture of the lip, collar and basal ring neuropil originate from varying size of microglomeruli, small spherical subunits which represent zones of synaptic contact between MB extrinsic and intrinsic neurons (Rybäk, 1994; Ganeshina and Menzel, 2001; Gronenberg, 2001) and the arrangement and morphology of the MBs approximately 170,000 intrinsic neurons, the Kenyon cells (Kenyon, 1896; Withköft, 1967). In the honeybee two principal classes of Kenyon cells (KCs) can be described, type I cells with their somata filling the cup-like structure the calyces are forming and type II KCs which have their somata located at the outside wall of the calyces, forming claw-like dendritic arborizations and therefore are also called clawed Kenyon cells (Rybäk and Menzel, 1993; Strausfeld, 2002; Fahrbach, 2006). The axons of the KCs of both calyces take a mutual route bifurcating towards the lobes thereby, extremely dense packed and organized in a parallel way, forming the pedunculus.

There are several more complex connections within the MBs, in particular a group of output neurons, having their soma lying in the A3 cluster that project back from

the lobes to the calyces via the protocerebral calycal tract (PCT) and seem to be inhibitory as showing GABA-like immunoreactivity (Bicker et al., 1985; Grünwald, 1999; Ganeshina and Menzel, 2001). The octopaminergic VUM_{mx1} neuron which is reacting to a sucrose stimulus is innervating the lip an basal ring within the MB and seems to convey the US during olfactory associative learning procedures (Hammer, 1993).

2.3 The honeybee as a model

Its comparable small number of neurons of approximately 900,000 (Witthöft, 1967) but highly structured brain, its capabilities of different types of learning and forms of memory, its complex social behavior and its high evolved sensory abilities, make the bee an optimal model organism for the various disciplines of neurobiology, from the nervous systems morphology to navigation cues and different learning tasks. Furthermore the finding and analysis of the VUM_{mx1} (Hammer, 1993) shows how the honeybee serves to make the connection between learning and the underlying cellular morphology. This individual identified neuron which is exhibiting activity upon a sucrose reward to the animal could be shown to convey the US of an olfactory conditioning task by replacing the sucrose reward with either a depolarization of the neuron or injecting octopamine, its putative neurotransmitter, into the brain areas it is projecting (ALs&MBs) (Hammer and Menzel, 1998; Reviews: Hammer, 1997; Menzel, 2001; Menzel and Giurfa, 2001, 2006). Another advantage of this rather small brain is that its volume makes it possible to work with whole mount preparations which can be dissected optical by using laser scanning or two photon microscopy and thereby keeping the brain and its neuronal networks intact.

2.4 Aim of this study

Differences between l- and m-ACT PNs are described on a physiological and morphological level in several studies. Müller et al. (2002) and Krofczik (2006) found differences in the response characteristics between neurons of both tracts and suggested the parallel olfactory pathways to code either different features of the same odor (Müller et al., 2002) or that one (m-ACT) codes for odor identity whereas the other (l-ACT) conveys mixture related information (Krofczik, 2006). On a morphological level Kirschner et al. (2006), by staining the whole tracts, found both tracts not only to be segregated by the AL glomeruli they innervate but also by projecting to separate regions in the MB lip and the LH. Abel et al. (2001) found complex innervation patterns of single cells within the MB lip and Krofczik (2006) suggested l-ACTs to innervate a central core of, and m-ACTs to show different bouton densities along the lip, based on 3D reconstructions of three single cells. In *Drosophila melanogaster* individual PNs were shown to have highly stereotyped branching patterns in MB and LH and that PNs innervating the same glomerulus also show similar axonal projections (Marin et al., 2002; Wong et al., 2002; Lin et al., 2007).

The aim of this study was to get further insight in the innervation pattern of single l- and m-ACT neurons of the honeybee. Therfore staining of individual cells was performed in order to analyze their glomerular origin, axonal projections and morphological differences based on confocal image stacks and 3D reconstructions. Furthermore in collaboration with the Zuse Institute Berlin a method for the computer based analysis of 3D reconstructed morphological data was evolved in order to be able to extract and compare anatomical features of single neurons.

3 Material and Methods

3.1 Animals

Worker honeybees (*Apis mellifera*) were caught at the hive entrance from March to September, using a plexiglass pyramid which was held in front of the hive entrance. Thus it was assured to catch only foragers.

3.2 Preparation

The animals were immobilized at 4 °C on ice and put into recording chambers. The head was fixed to the chamber using a drop of low melting dental wax on each eye and a piece of overhead transparency behind the neck.

Mounted animals were kept in the dark at 20-25 °C and high humidity and fed with 35 % sucrose solution. Bees were used for experiments up to three days after they were catched.

Right before the staining procedure the antennae were fixed with a drop of low

melting eicosan and a window was cut into the head capsule between the compound eyes, the medial ocellus and the scapi of the antennae. A second triangular window through which the esophagus was overstretched was cut above the mandibles. The mandibular muscles were cut and the abdomen slightly squeezed with plasticine to prevent brain movement caused by hemolymph pumping or muscle contraction. Trachea covering the staining side and hypopharynx glands were carefully removed. To prevent the brain from running dry the esophagus hole was sealed with eicosan and a drop of bee Ringer solution was put onto the brain if needed.

3.3 Intracellular staining

Intracellular stainings were performed with electrodes pulled from borosilicate glass capillaries (length: 75 mm, inner diameter: 0.53 mm, outer diameter: 1.0 mm, wall thickness: 0.21 mm; Hilgenberg GmbH, Malsfeld, Germany) using a P97 horizontal puller (Sutter Instrument Company, Novato, CA).

The electrode tips were filled with 10 % NeurobiotinTM (Vector Laboratories Inc., Ontario, CA) diluted in 0.2 M potassium acetate. Resistances in the tissue ranged from 60 MΩ up to 200 MΩ. Electrodes were inserted into the antennal lobe in different depths to stain either l-ACT neurons innervating the more anterior-dorsal T1 area, or m-ACT neurons innervating the more posterior-ventral areas T2-T4. A chlorized silver wire placed into the compound eye served as the indifferent electrode.

When a stable recording could be observed on the oscilloscope the NeurobiotinTM was iontophoretically injected into the cell by applying a depolarizing current of 1-4 nA to the electrode for at least 5 min, either constant or in pulses of 1-2 Hz and 0.2 s

duration, depending on the electrode's resistance. After injection wax and plasticine were removed, bee Ringer put onto the brain and the bees were put back into the dark to let the Neurobiotin™ diffuse for 1-4 h to ensure a complete filling of the cell.

Afterwards, the head was cut off and fixated in 4% paraformaldehyde in phosphate buffered saline (PBS, pH 6.7) at 4 °C over night. On the next morning the brains were dissected, freed from all trachea, washed in PBS 3 times for 10 min and incubated for 2 h in 0.3 % Triton X in PBS at room temperature in order to get the cell membranes permeable for the streptavidin conjugated fluorescent dye, Cy5 (Jackson ImmunoResearch Europe Ltd., Suffolk, UK). Brains were then incubated in 500 µl PBS containing 1 µl streptavidin-Cy5 (1:1 in glycerol), 1 µl NaAcid and 1 µl Lucifer Yellow over night at 4 °C. The Lucifer Yellow was used for the neuropil counter staining. The next day the brains were washed in PBS 4 times (15 min, 30 min, 45 min, 60 min), dehydrated in an ascending ethanol series (50 %, 70 %, 90 %, 99 %, 100 %; 10 min each step) and then mounted as whole mounts in methyl-salicylate on custom double-sided slides.

3.4 Confocal microscopy

Confocal image stacks were acquired with a confocal laser scanning microscope (Leica TCS SP2) using either a 10x0.4 IMM lens objective or a 20x0.5 water lens objective. Per stack, around 400 sections were scanned with a resolution of 1024x1024 voxels each, and with a voxel size of 0.61 x 0.61 x 1.3 µm or 0.73 x 0.73 x 1.1 µm. The neuron- and background channel were sampled in parallel, Cy5 was excited at 633 nm using a HeNe Laser, Lucifer Yellow was excited with the 488 nm line of an argon-ion

laser. A linear intensity compensation was used to adjust differences in brightness depending on scanning-depth.

3.5 Reconstruction

All 3D reconstructions were done with Amira (Mercury Computer Systems, Inc, San Diego, CA). Reconstruction of projection neuron morphology was performed on confocal image stacks by using a custom module (Schmitt et al., 2004; Evers et al., 2005). On those reconstructed SkeletonTrees individual vertices were labeled as boutons. Neuropils were reconstructed out of the neuropil image stack by tracing its borders with Amira's build in segmentation editor.

3.6 Data evaluation

3.6.1 Image & data processing

Images were acquired using Amira and, if needed, adjusted in size and resolution with Adobe® Photoshop® Elements 2.0 (Adobe Systems Inc., San Jose, CA). All figures were created using OpenOffice.org Draw 2.3.1 (Sun Microsystems Inc., Santa Clara, CA).

Calculations were performed and all histograms computed using OpenOffice.org Calc 2.3.1 (Sun Microsystems Inc., Santa Clara, CA).

3.6.2 SkeletonTree

Neuropil labels were mapped onto SkeletonTrees as to give every vertex an ID according to the neuropil it resides in. Informations on SkeletonTrees were exported to OpenOffice.org Calc as spreadsheet using the build in SkeletonStats module and with this data a boutons belonging to a neuropil could be extracted.

3.6.3 Lip zones

Surfaces of the lips were calculated based on the generated label field and then manually dissected using Amira's build in path editor. The EvaluateBoutons module by Anja Kuss from the Zuse Institute Berlin was used to calculate a boutons belonging to one of the zones created and data was exported to Open Office Calc as spreadsheet for further analysis. The zones applied are illustrated in figure 2 A.

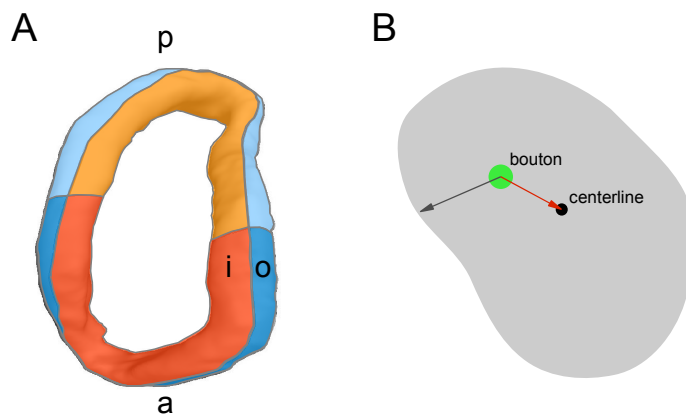


Figure 2: Scheme of zones applied to the lip and vectors for calculating bouton distances. **A:** MB lips were manually dissected into four zones: inner-anterior, *dark orange*; inner-posterior, *light orange*; outer-anterior, *dark blue*; outer-posterior, *light blue*. **B:** Cross section through a lip illustrating the two vectors measured for each bouton: *green dot*, bouton; *black dot*, centerline; *red arrow*, shortest distance to centerline; *dark gray arrow*, shortest distance to neuropil surface.

3.6.4 Bouton distribution

A centerline for each lip surface model was calculated using Amira. The EvaluateBoutons module was used to calculate two vectors for each bouton, its shortest distance towards the centerline and the lips surface. With the lengths of these two vectors a relative distance from the centerline was calculated for every bouton according to the following equation:

$$\frac{distance_{centerline}}{distance_{centerline} + distance_{surface}}$$

3.7 Used solutions

Bee Ringer:

| | [mM] |
|-------------------|------|
| NaCl | 130 |
| KCl | 6 |
| MgCl ₂ | 4 |
| CaCl ₂ | 5 |
| Hepes | 10 |
| Glucose | 25 |
| Sucrose | 170 |

set to pH 6.7 with NaOH/HCl

PBS (phosphate buffered saline):

| | [mM] |
|---|------|
| NaCl | 37.0 |
| KCl | 2.7 |
| Na ₂ HPO ₄ | 8.0 |
| KH ₂ PO ₄ | 1.4 |
| 1 volume + 4 volumes H ₂ O dest. | |
| set to pH 7.2 with NaOH/HCl | |

4 Results

The antennal lobes (AL) get input from the antennae by olfactory sensory neurons (ORN) that project by means of four antennal tracts (T1-T4, Suzuki 1975) towards the 156 spherical AL subunits, the glomeruli. Each antennal tract is innervating a specific subset of glomeruli which are hereby clustered into four groups (Flanagan and Mercer, 1989; Galizia et al., 1999a). Information from the ALs is conveyed to higher order brain centers via five tracts. Two of them, the lateral and medial antennocerebral tract (ACT) are uniglomerular, innervating only one glomerulus, and have their axonal branches in the lateral protocerebral lobe (LPL) and the mushroom bodies (MBs) (Abel et al., 2001). The remaining three mediolateral ACTs send their dendrites to multiple glomeruli and arborize in the LPL only (Kirschner et al., 2006).

In this study, eight single cell stainings of uniglomerular projection neurons (PNs) were evaluated, four belong to the lateral antennocerebral tract (l-ACT) and four to the medial antennocerebral tract (m-ACT) (Fig. 3). Projections of these neurons in the mushroom body (MB) have been completely traced and reconstructed and bouton-like swellings were marked individually within the 3D SkeletonTree models (see methods). Each single stained neuron is referred to as M1-M4 or L1-L4 with respect to their origin in the antennocerebral tracts (ACT) and numbered according

to their staining history. From six neurons (Fig. 3 C-H) the respective innervated glomerulus in the antennal lobe (AL) and the appropriate soma could be identified (Fig. 4 and table 1). In three of the l-ACT stainings more than one neuron was filled but only one completely, thus the observed innervations in the calyces were always restricted to a single individual cell but innervation of the lateral horn might arise from more than one.

Positions of neurons are described relative, with respect to the enclosing neuropil as fixing and staining procedure led to different amounts of shrinking. Some figures were flipped horizontally and hereby transformed to the other brain hemisphere for better comparability, flipping is indicated by a dot in the lower left corner.

4.1 Innervation of the antennal lobe

In three out of the four l-ACT preparations additional cells were observed leaving the AL via the l-ACT. These neurons are always less intense in their coloration and in most cases the tracer did not even run as far as the mushroom bodies, indicating either an indirect loading with NeurobiotinTM or hitting the cell only shortly. Interestingly this phenomenon could not be observed for the m-ACT stainings. In nearly all stainings additional neurons can be seen, most of them local interneurons which were hit along their course through the AL tissue.

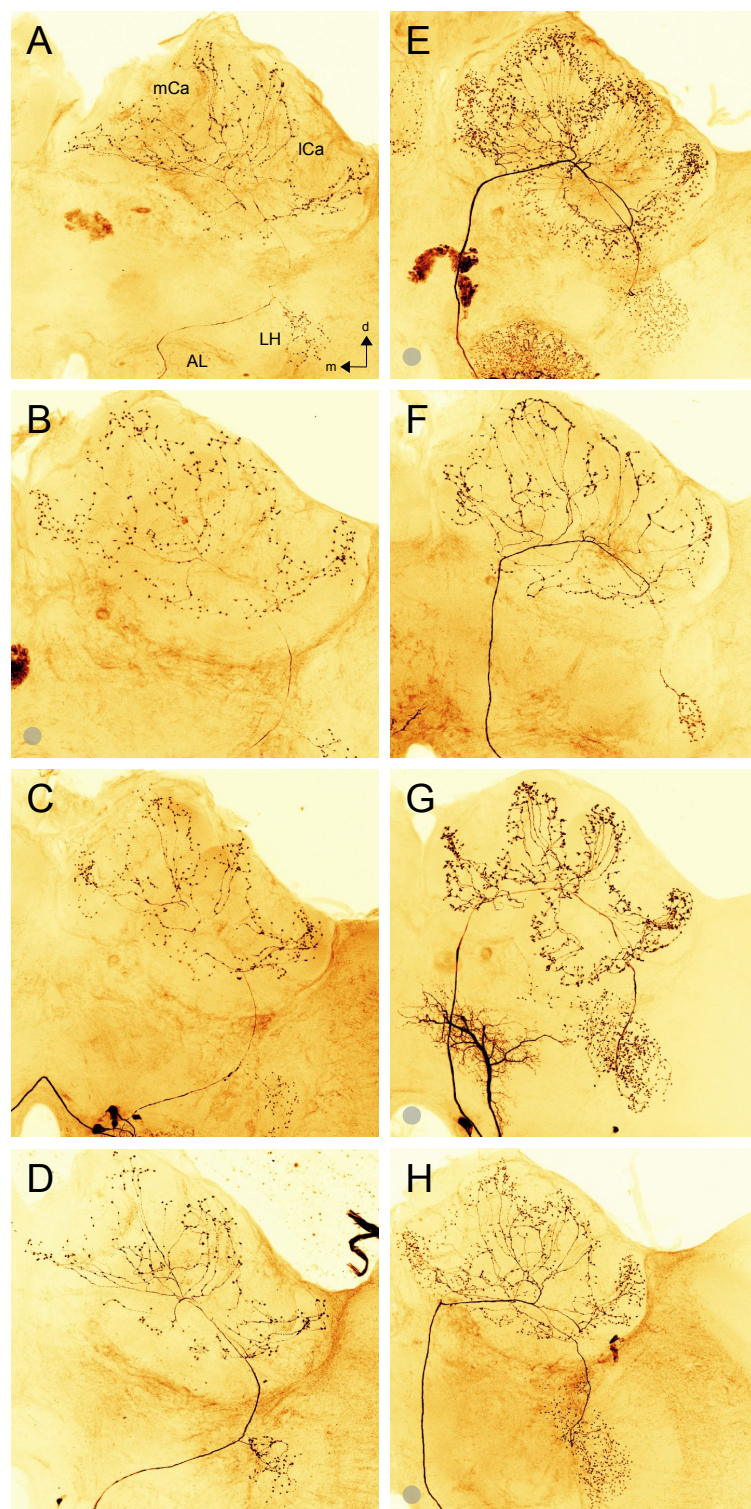


Figure 3: Projection views of individually stained neurons. Left column shows the PNs of the 1-ACT, the right column those of the m-ACT. Individual neurons are referred to as L1-4 (A-D:) and M1-4 (E-H:) named by their belonging to either of both tracts and the time of staining. A gray dot indicates horizontally flipping of the picture.

4.1.1 Glomeruli

Six innervated glomeruli out of eight preparations could be identified using the digital antennal lobe atlas from Galizia et al. (1999a) and the work from Kirschner et al. (2006). Identified glomeruli from l-ACT preparations could be assigned to the T1 cluster (Fig. 4 A and B), m-ACT neurons projected to glomeruli of the T3c (Fig. 4 F) and the T4 cluster (Fig. 4 E,G and H and table 1).

The neuron M2 (Fig. 3 F and 4 D) is innervating a glomerulus that can be found as D07 belonging to the T4 group in the Galizia atlas but is described as glomerulus C73 belonging to the T3c cluster by Kirschner, here the nomenclature by Kirschner et al. (2006) is used as the other m-ACT neurons stained innervate T4 glomeruli and differ in their morphology. According to Kirschner et al. (2006) two glomeruli, D01 and D02, are innervated neither by m- nor l-ACT neurons, here the neuron M3 was found to project to D02 (Fig. 3 G and 4 E).

4.1.2 Soma location

Somata of two l-ACT PNs could be allocated to a broad cluster described in Kirschner et al. (2006) and Abel et al. (2001) with regard to their position in the AL (Fig. 4 A and B). M2's soma was found to belong to the mSC2 cluster 'situated medially (Kirschner et al., 2006) (Fig. 4 D). However, the somata of neurons M1, M3 and M4 located also at the medial side of the AL (like clusters mSC2 and mSC3) but far more ventral matching a bundle shown by Abel et al. (2001, Fig. 2) and suggesting a fourth cluster of m-ACT somata (Fig. 4).

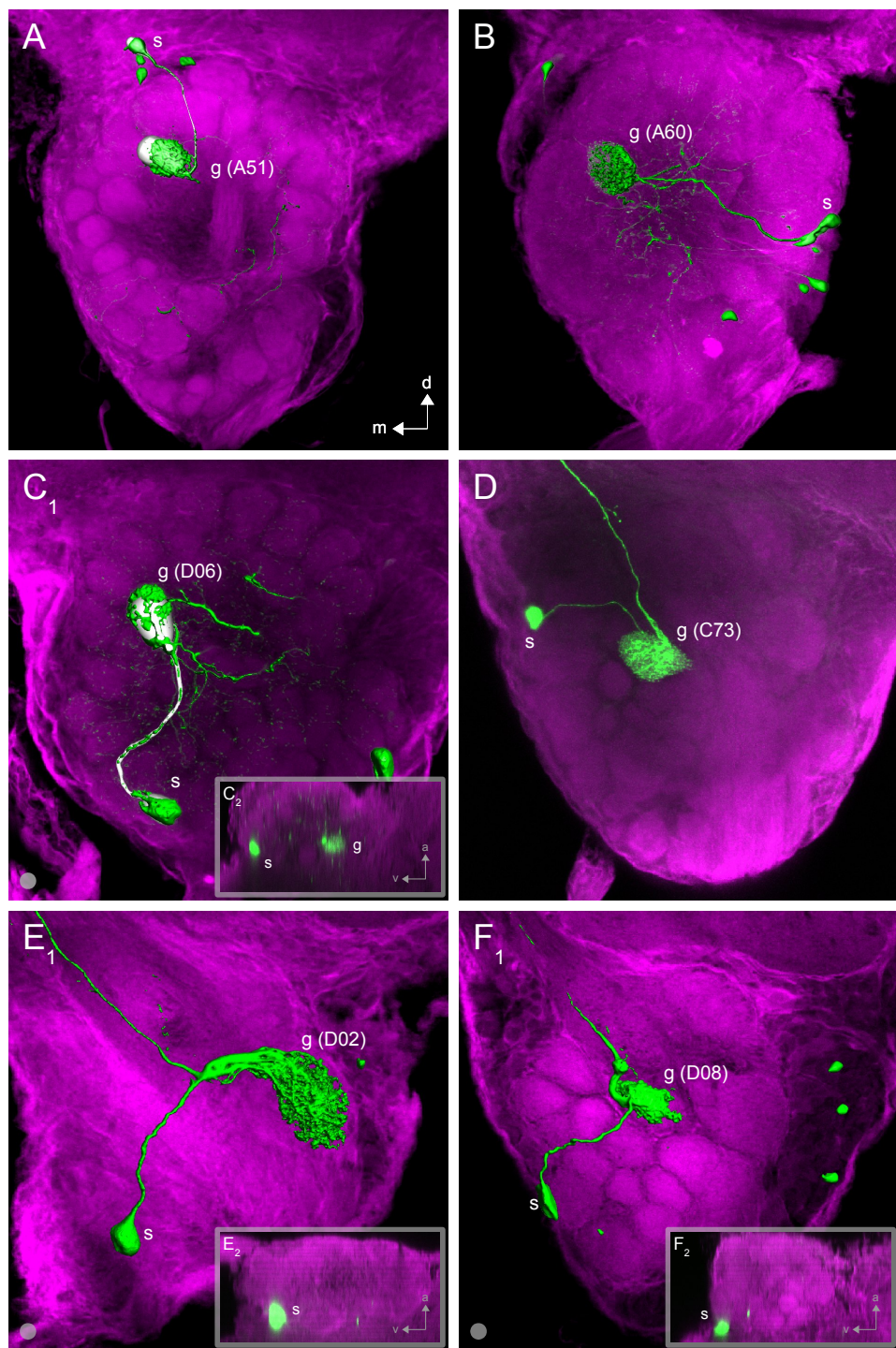


Figure 4: Identified glomeruli of PNs. Glomeruli and somata are visualized as isosurfaces and in A and C additionally as SkeletonTrees. ALs are displayed as projection views of a few sections in glomerulus depth (z-axis). C₂, E₂ and F₂ show sagittal views to describe soma locations. A and B show preparations L3 and L4, C-F preparations M1-M4. A dot in the lower left corner indicates that the image was flipped horizontally to increase comparability. *g*, glomerulus; *s*, soma.

4.1.3 Arborizations

For two m-ACTs and one l-ACT neuron arborizations within the ALs were found (Fig. 5). While M2 is splitting off two small branches short before entering the tract and leaving the AL, M3 is sending a larger, more complex ramifying one remote from the innervated glomerulus (Fig. 5 A and B). L3 shows a similar branching pattern like M2 sending off two extensions directly before entering the bundle which leaves the AL (Fig. 5 C). These branches are all located in glomeruli free regions making it unlikely that they are innervating additional glomeruli. Similar observations were made by Müller et al. (2002).

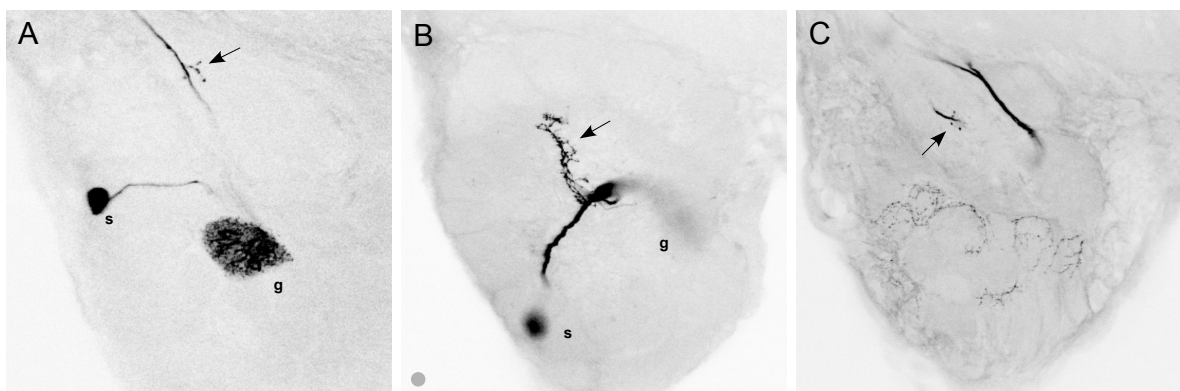


Figure 5: AL sections of two m-ACT and one l-ACT. **A:** Axon of the neuron M2, ramifying close to the AL exit of the m-ACT, forming blebs (arrow). **B:** Axon of M3 is splitting off larger, more complex, branches directly before entering the glomerulus. **C:** L3 shows short branches with blebbly structures like M2. *s*, soma; *g*, glomerulus.

4.2 Innervation of the mushroom body

4.2.1 Branching pattern

Projection neurons reach the pedunculus from its lateral (l-ACT) or medial (m-ACT) side, depending on the tract they belong to, and run around the pedunculus necks where they send off collaterals heading towards the two inner ring tracts (IRTs, Mobbs 1982) of each mushroom body (Fig. 7). One or two branches per calyx hemisphere enter from anterior, run along the inner rim of the basal ring and meet but do not close at the posterior calyx side (Fig. 7 A). On their circling route they send off several collaterals which might divide again and finally enter the lip.

The stained l-ACT neurons access the lip with 12 to 15 branches per calyx, arising from the IRT, each innervating a distinct lip segment where it arborizes further. Each innervated field is separated from its neighbor by a rather big gap (6 A-D). Neuron M2 reveals similar structural properties whereas M3 and M4 send off 20 to 27, M1 around 40 ascending collaterals per calyx from the IRT. Domains are clearly separated and do not extend in lateral (with respect to the longitudinal axis) zones in the l-ACTs and M2, but touch or even overlap within the other m-ACT neurons which innervate the lip continuously all around (Fig. 6).

4.2.2 Boutons

The main innervation area of all stained olfactory projection neurons within the mushroom body calyces is the lip neuropil. This is represented by the intensive amount of axonal ramification and the high number of bouton-like presynaptic

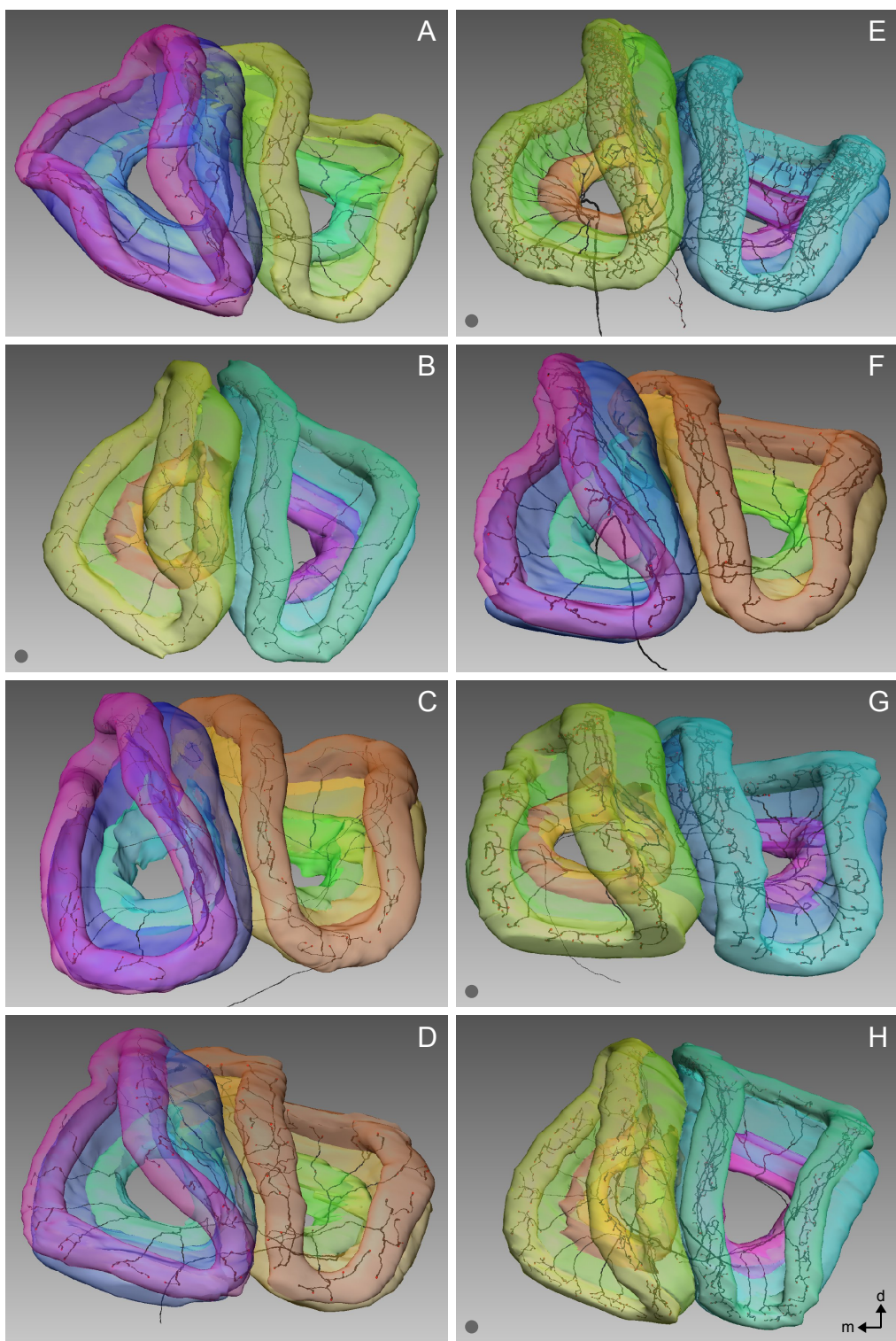


Figure 6: SkeletonTrees of reconstructed neurons within the calyx neuropil. **A-D:** Preparations L1-L4. **E-H:** Preparations M1-M4. Altered colors are due to different material IDs of the underlying label fields and have no further meaning. A Gray dot in the lower left corner indicates that the image was flipped on its x-axis for better comparability.

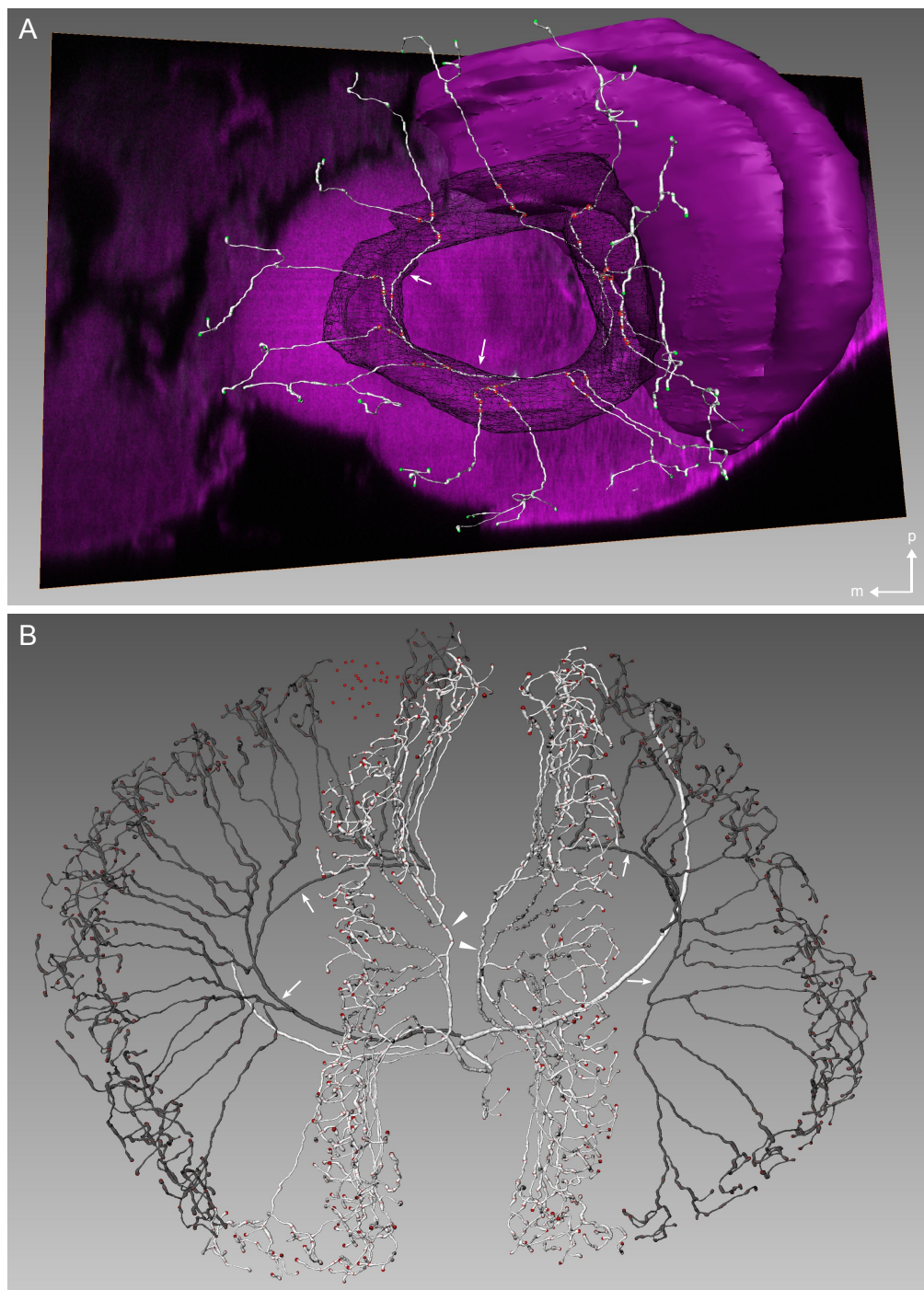


Figure 7: Dorsal views of an l- and an m-ACT projection in the calyx neuropil. **A:** View inside the medial calyx of preparation L1, arrows indicate the neuron running through the IRT, medial basal ring (BR) is shown as grid, boutons are green, boutons within the BR are marked red. **B:** SkeletonTree showing calyx innervation of neuron M1, lateral hemispheres in dark gray. “Free flying” boutons in the posterior part of the lip are due to a cut in the preparation. Arrows point at neuron running through the lateral part of IRT arrowheads at medial.

swellings expressed in this area. In general boutons occur in three positions at the cell, along the way as *en passant* blebs, at branching points, here called axillary blebs (arrows in figure 8 A and C), and at the axon terminal. Three m-ACT neurons (M1, M2 and M3) show big rosette-like boutons which were found exclusively within the lip, where M2 shows rounder boutons like all l-ACTs in this study do (Fig. 8 B and C). Boutons of all stained PNs sometimes form additionally spiny structures in the lip (arrow heads in figure 8 A) but not in other neuropils. In the l-ACT preparations lots of further tiny blebs can be seen between the normal boutons (Fig. 8 B).

By branching off from the IRT and sending collaterals towards the lip, axons cross the basal ring neuropil where they form *en passant* blebs which are smaller as the boutons within the lip (white arrows in figure 8 E). Additional boutons could be found in the collar region adjacent to the lip, described as distal collar in Gronenberg (2001). This region can not be seen in the Lucifer Yellow counter staining (Fig. 8 D₁) but is clearly visible in the NeurobiotinTM/Cy5 channel as a darker stripe (Fig. 8 D₂ and E).

Bouton count

Differences were found with regard to the number of boutons within the lip comparing all different projection neurons stained. All bouton counts can be found in table 1. The stained PNs possess less boutons in the medial lip than in the lateral, within both lips the complete l-ACTs bouton count ranges from 166 to 327. More variance can be found in the m-ACT PNs. Here the lowest bouton count is 324, two in the mid range had 513 and 616, and the neuron M1 with the most boutons found expressed 1331 swellings (Fig. 7B).

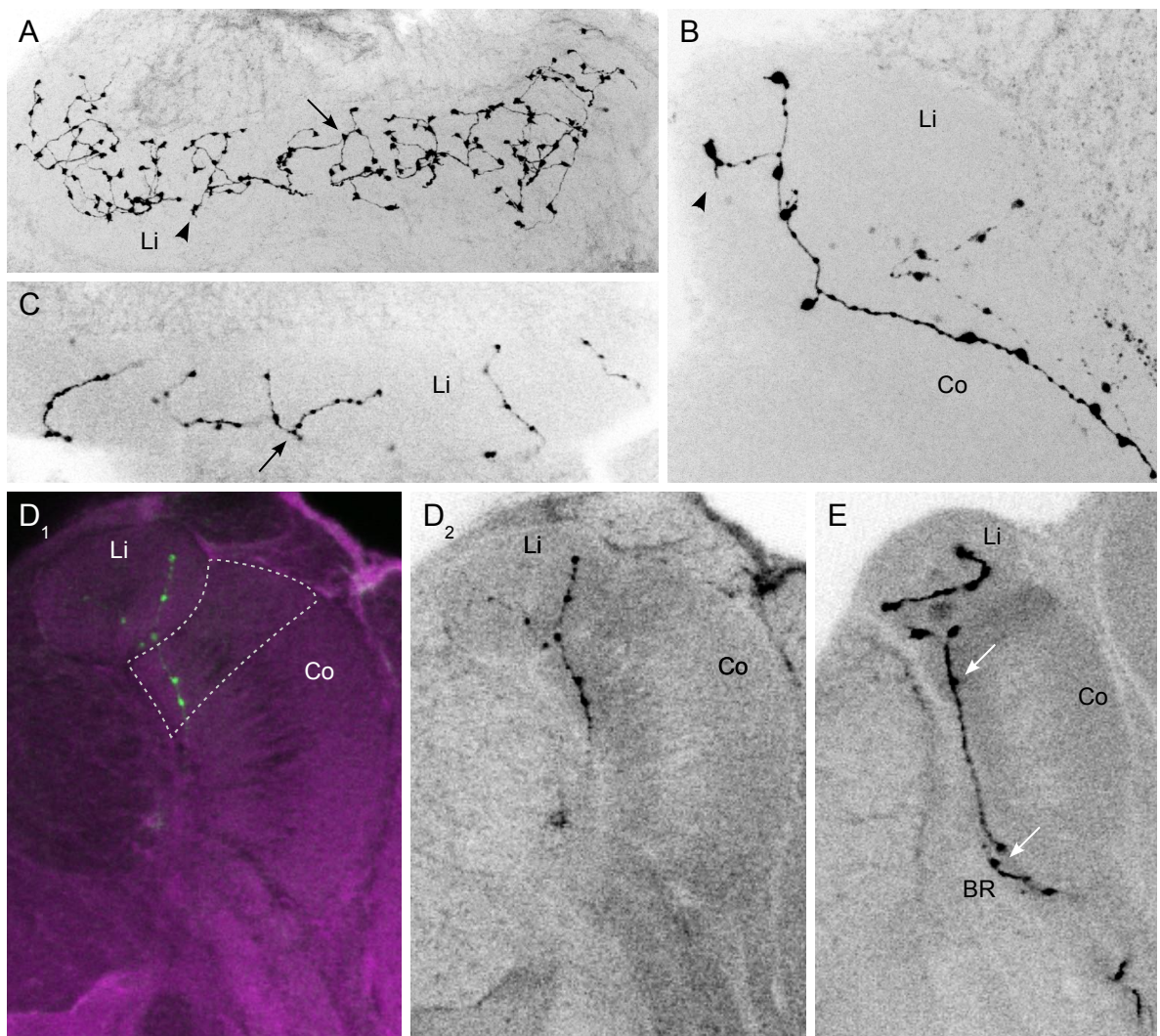


Figure 8: Boutons in the mushroom bodies. **A-C:** Projection views of a few sections of the lip. **A** and **C** show m-ACT projection neurons (M1 and M2), **B** displays a l-ACT neuron (L1). **D-E**, are single sections through a calyx, **D** is an l- **E** an m-ACT neuron. *BR*, basal ring; *Co*, collar; *Li*, lip; *black arrows*, axillary blebs; *arrow heads*, spiny extensions; *white arrows*, *en passant* blebs outside the lip; *dashed line*, distal collar region.

4.2.3 Bouton distribution within the lip neuropil

As individual boutons were marked within the SkeletonTree of the neuron several new modes of spatial analysis were applied. To identify possible sub zones of innervation in the lip, the surface was dissected into four zones according to figure 2 using the path editor, boutons were assigned to the so created zones and counted. Boutons accounted to the inner lip can be seen in red in figure 9 A, boutons in yellow belong to the outer lip. The dissection of the lip was performed with respect to findings of previous studies which found either axonal PN (Abel et al., 2001; Kirschner et al., 2006) or dendritic Kenyon cell (Strausfeld, 2002) arborizations restricted to according zones. Additionally the shortest distance between each bouton, a calculated neuropil centerline and the surface was measured and the relative distance from the centerline was calculated (Fig. 9 B).

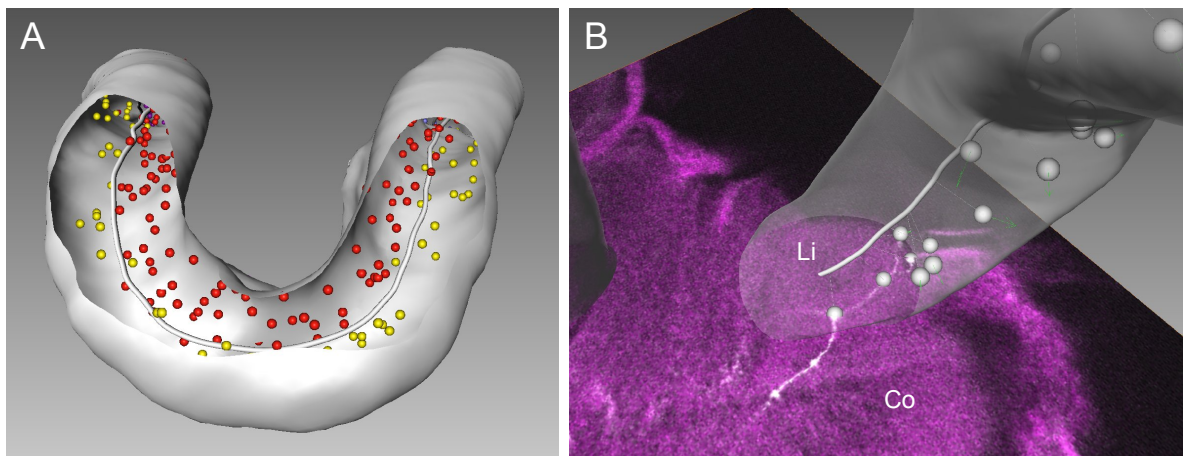


Figure 9: Boutons within the reconstructed neuropil. **A:** Anterior part of M1's lateral lip, boutons are assigned to either the inner (red) or the outer lip (yellow). **B:** Part of L4's medial lip showing boutons located at the peripheral lip, green arrow indicate the shortest distance towards the surface, gray lines the shortest distance to the centerline. *Li*, lip; *Co*, collar.

Manual dissection of the lip

Each lip was manually sectioned in 4 zones, an inner and an outer zone which were further divided in their anterior and posterior parts (Fig. 2 A). The results of the bouton density analysis are shown in figure 10 and were additionally color coded and visualized in figure 11.

L-ACT neurons First of all l-ACT PNs (left column in figure 10 and 11) show a continuous innervation pattern, innervating either the inner or the outer lip of both calyces more intense (white and gray bars in figure 10 A-D). An equal rate of boutons in the anterior and posterior parts is consistent for all l-ACT PNs too (striped bars in figure 10 A-D).

Nevertheless there are differences in bouton density between the anterior and posterior lip if comparing the inner and outer regions separately, most obvious in the inner part of the lateral lip of L1 (orange bars in figure 10 A) and the outer parts of L2's medial lip (blue bars in figure 10 B). Lateral and medial calyx lips of the stained l-ACT neurons show the same gross innervation pattern in all cases. Except for L3 (Fig. 10 C and 11 C) all l-ACT PNs exhibit a bouton count in the outer lip that is around two times higher than in the inner part (eight times in L4's medial lip, figure 10 D), in L3 it is opposite.

M-ACT neurons The bouton distribution of three stained m-ACT PNs within the lip is more complex and does not exhibit a steady pattern as shown for the l-ACT PNs (right columns in figure 10 and 11). In contrast one neuron, M4 (Fig. 11 H), shows a clear segregation in an outer and an inner zone like the l-ACTs do. Conspicuous

accumulations of boutons can be observed in the inner anterior zone of M1's lateral lip (Fig. 10 E, 11 E and 9 A) the innervation of the other three zones is equal. In the medial lip however, the whole inner region shows a higher count of boutons compared to the outer lip. M2's lateral lip exhibits a peak of boutons in its outer posterior zone (Fig. 10 F) which can not be seen in the medial lip, but there is still a pronunciation of the posterior parts. For M3 (Fig. 10 G) it is opposite, here a peak in the outer posterior zone can be observed in medial lip which can not be seen in the lateral lip where differences are not that high. M4 as mentioned before reveals an innervation pattern that resamples most of the stained l-ACTs with an accumulation of boutons in the outer zones of both, lateral and medial lip.

Bouton distance from centerline

The second approach to analyze bouton distribution was to classify the boutons position within the lip according to two vectors, the shortest distance towards the lips centerline and the shortest distance towards the neuropil surface. The length of these vectors was used to calculate each boutons relative distance to the centerline, thus a value between 0 and 1 was accounted to every single bouton (see 3.6.4 and figures 2 B & 9 B). The histograms in figure 12 show the relative number of boutons per lip, binned into ten equal wide classes (10 % each) from 0 (centerline) to 1 (surface).

Within a single neuron the bouton distribution, with respect to the pattern, is equal between the two innervated lips. Higher variances can only be seen in neuron L1 and L4 (Fig.12 A₂ and D₁) where either one lip shows a larger peak than the other, the peak position however stays the same.

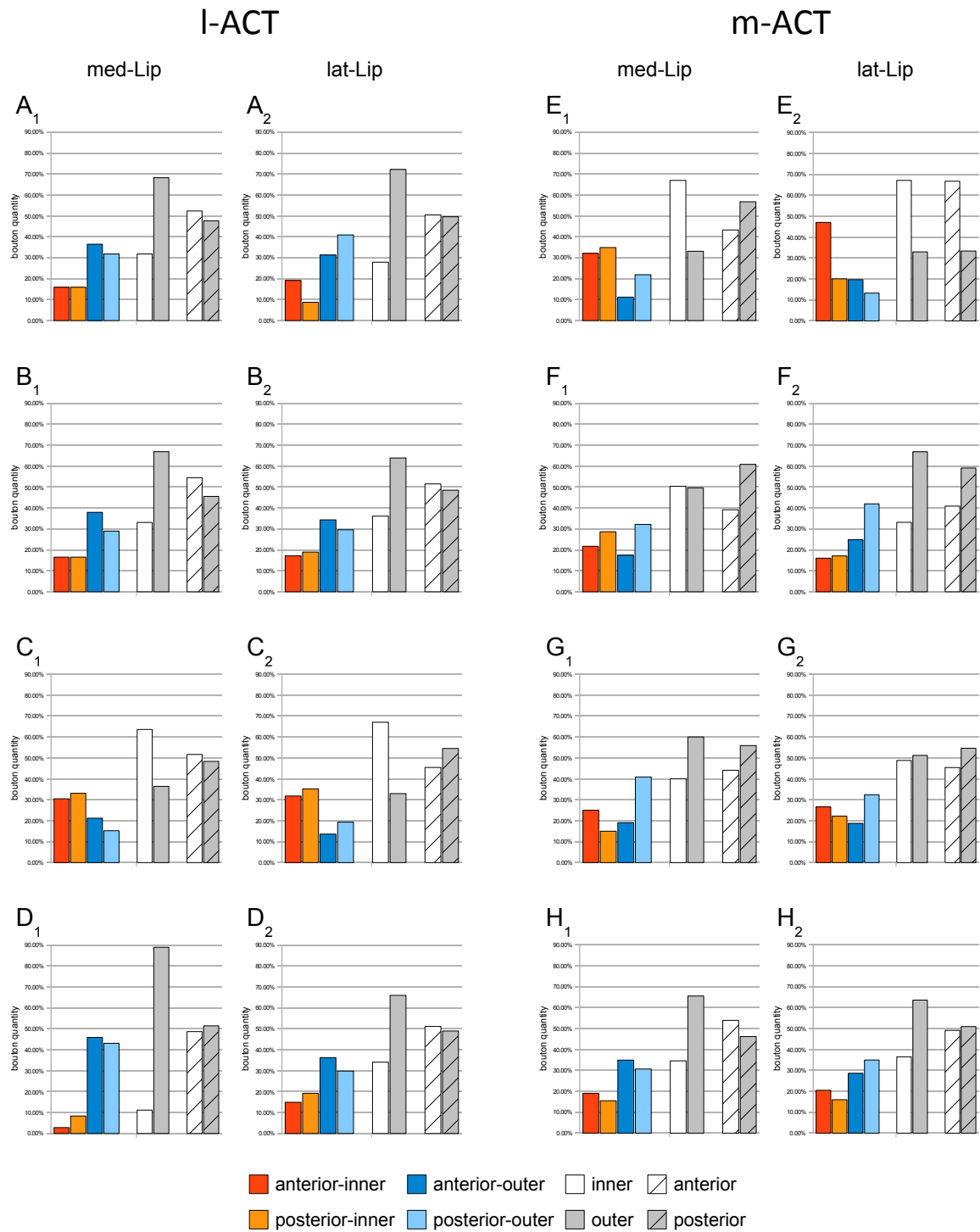


Figure 10: Bouton count in four manual sectioned zones. **A-D** show I-ACT neurons L1-L4, **E-H** neurons M1-M4. Bouton quantity is displayed in percent of boutons of the corresponding lip.

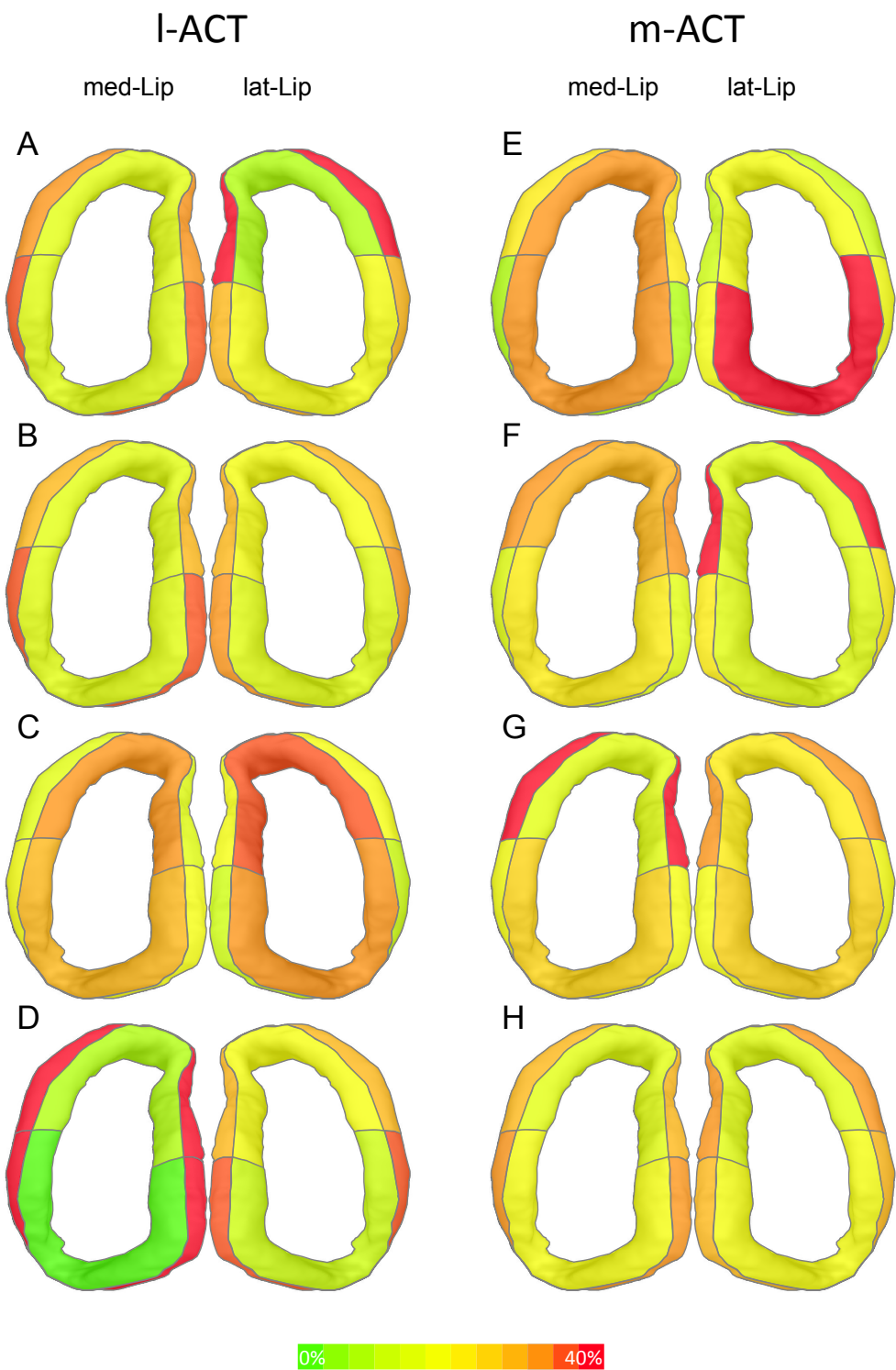


Figure 11: Color coded scheme of bouton count in four manual sectioned zones. **A-D** show schemes for preparations L1-L4, **E-H** for preparations M1-M4. Zones are described in figure 2 A.

L-ACT neurons Neurons L1 and L4 have only a minority of boutons located in the first two or three bins, thus next to the centerline, but most of them in the periphery (Fig. 12 A and D). L3 also has relative few boutons in the first two central bins but shows no clear peak in the outer zones, instead reveals a rather homogeneous distribution in its medial lip (Fig. 12 C₁) and a steadily rising number of boutons toward the periphery in its lateral lip (Fig. 12 C₂). In L2's medial lip, a rising number of boutons towards a peak in the middle between centerline and surface which is falling again towards the periphery, can be observed (Fig. 12 B₁). In the corresponding lateral lip (Fig. 12 B₂) a similar distribution in the first five bins can be seen but the number of boutons is not as steadily falling towards the periphery as in the medial lip.

M-ACT neurons M-ACT PNs M1 and M2 (Fig. 12 E and F) exhibit one clear peak in bouton distribution with M1 having its bouton maximum oriented at the outside of the lip and M2's in the middle between centerline and surface. Both distributions rise and fall steady from centerline to surface, having their minimum in the bins adjacent to the centerline. Comparing M2's lateral lip with the medial, the peak is slightly shifted towards the periphery. M3 shows no clear peaks in its lips, boutons are broadly distributed between the central and the peripheral lip with minima in the bins next to the centerline and the surface (Fig. 12 G). In the medial lip of M4 the bouton density is again almost steadily rising towards a maximum in the bin that covers the 70% to 80% distance from the centerline and going down in the two bins next to the surface (Fig. 12 H).

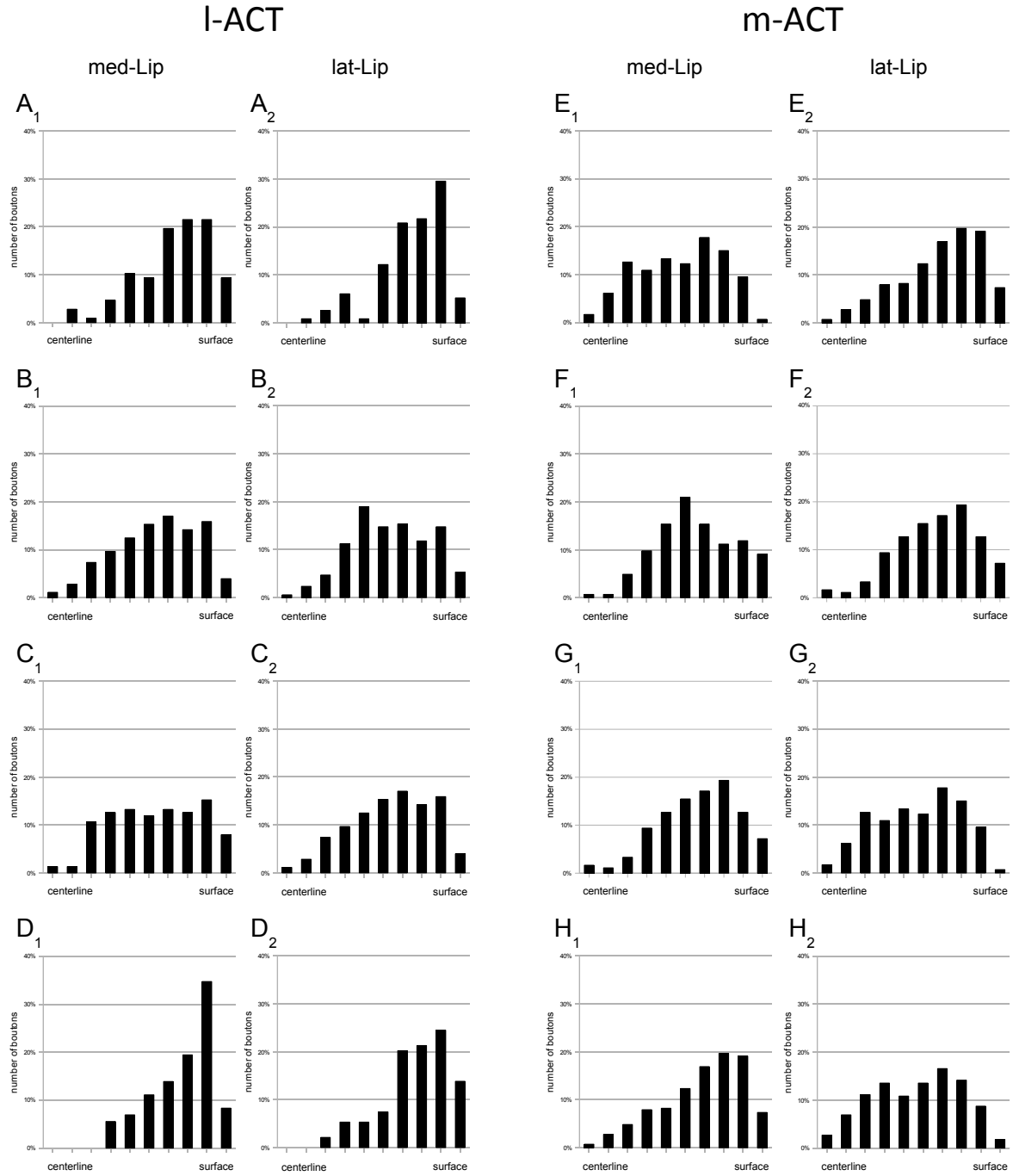


Figure 12: Relative distances from the centerline. Histograms show the distribution of boutons in the lip with regard to their location between the centerline and the surface. Boutons are binned in ten classes of equal width. Bouton quantity is displayed as relative amount in relation to all boutons of the single lip. **A-D:** I-ACT PNs L1-L4. **E-H:** m-ACT PNs M1-M4.

4.3 Protocerebral projections outside the MBs

In three m-ACT PNs short arborizations in the protocerebral lobe beneath the calyces were found (arrows in figure 13 A-C). In two of these preparations the protocerebral-calycal tract (PCT) was clearly visible in the background counter stainings ("PCT" in figure 14 C₁) and could be partly reconstructed which reveals that the neurons projections express boutons in close proximity to the tract (Fig. 13 D and E). Neuron M3 sends off a very thin branch in lateral and ventral direction before sending the first branch towards the IRT. This branch arborizes in the central protocerebral lobe (PL) posterior to the pedunculus where it is exhibiting several boutons (arrowhead in figure (13 B).

4.3.1 Lateral protocerebral lobe

Within the LPL all l-ACT neurons that were stained exclusively innervate the LH (Fig. 3 A-D) which is consistent to the findings of Abel et al. (2001) and Kirschner et al. (2006). Of the four m-ACT PNs three additionally arborize over a large area between LH and the pedunculus (Fig. 13 A-C and 14 C-E). One m-ACT (M2) however also innervates the LH exclusively.

All l-ACT and the one m-ACT projection in the LH were found to resample the zones described by Kirschner et al. (2006). The l-ACTs arborize in the outer part of the LH, shown to be the main projection area of l-ACTs and named zone #3 by Kirschner, only sparsely innervate the central zone and lack branches in the medial part (Fig. 14 A). The m-ACT is innervating the central LH, an area named zone #2 and shown to be innervated by PNs of both tracts (Fig. 14 B).

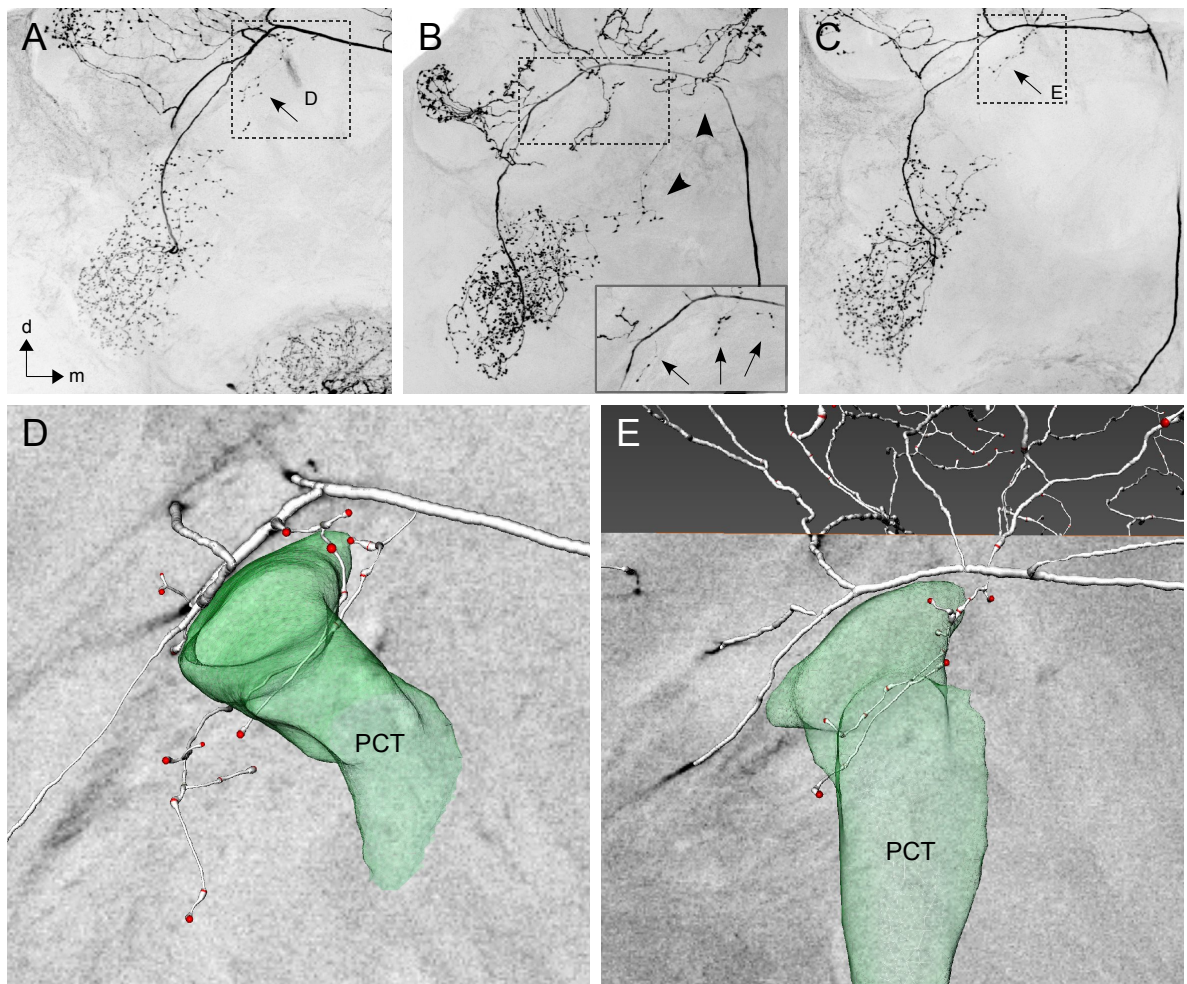


Figure 13: M-ACT PN arborizations outside the MB. **A-C** show projection views of m-ACT preparation M1, M3 and M4, arrows point at arborizations beneath the calyces, the arrowhead in **B** points at a very thin branch that is send off before the first branches project towards the IRT. **D** and **E** are magnifications from **A** and **C** and show the reconstructed neuron with boutons in red, in green transparent, part of the PCT as reconstructed from the Lucifer Yellow counter staining, is illustrated. *PCT*, protocerebral-calycal tract.

The remaining three m-ACT PNs reveal a different LH innervation pattern each. Figure 14 C-E show three consecutive sections of the anterior, medial and posterior parts of the respective LH. M1 was found to lack arborizations in the central part of the LH but innervates the remaining parts rather homogeneously (Fig. 14 C). M3 exhibits only a few arborizations in the outer rim (Fig. 14 D) whereas M4 broadly innervates the LH through its whole depth (Fig. 14 D).

LPL innervations outside the LH of these three neurons describe a wide band that reaches from the LH towards the pedunculus and provides an extensive amount of arborizations which carry a high number of boutons. In figure 14 D₃ the arrow points at three boutons located directly at the pedunculus rim. Unfortunately the branching in the LPL was too dense to allow a individual reconstruction at the given z-resolution of the used objective. For higher resolution objectives the branching occurs too deep as to scan it as a whole mount.

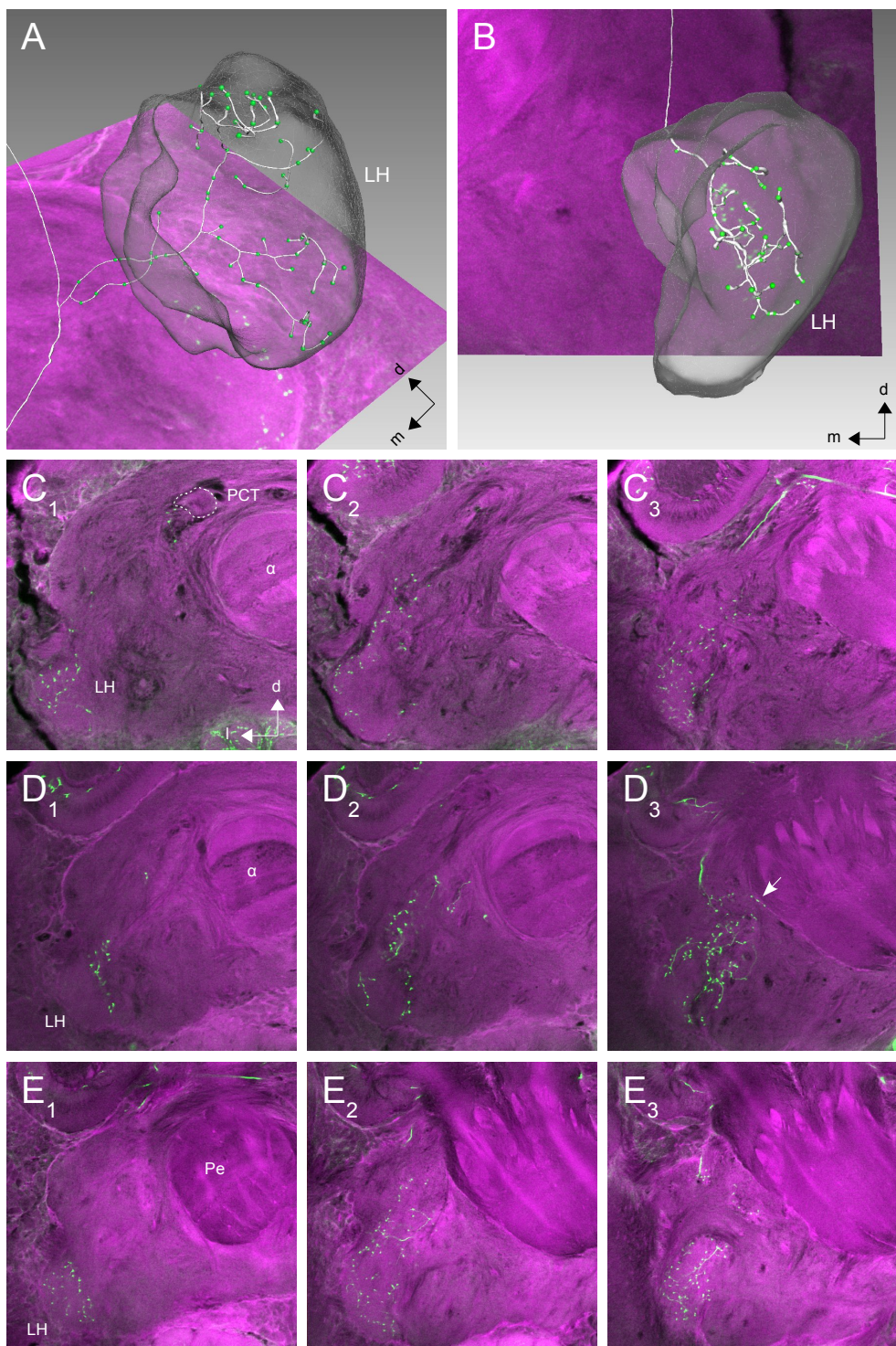


Figure 14: LPL projections. **A** and **B** display SkeletonTrees of neurons L1 and M2 inside the reconstructed LH, boutons are shown in green. To illustrate the LPL borders a projection view of a few slices was placed under the LH. **C-D** show consecutive slices through different depths of the LPL from anterior to posterior of three m-ACT preparations. **C:** M1, **D:** M3, **E:** M4. α , alpha lobe; LH, lateral horn; PCT, protocerebral-calycal tract.

Table 1: Summary of different features of the stained neurons. For L1 and L2 no individual glomerulus could be identified due to additional staining of several multiglomerular local inter neurons.

| neuron | glomerulus | cluster | boutons | | | | | | LPL projection | |
|--------|------------|---------|---------|------------------------|------------|-----|-------------------------|------------|----------------|---------|
| | | | lip | medial calyx collar | basal ring | lip | lateral calyx collar | basal ring | sum | |
| L1 | ? | ? | 107 | 25 | 40 | 115 | 25 | 30 | 342 | LH only |
| L2 | ? | ? | 145 | 15 | 25 | 169 | 23 | 18 | 395 | LH only |
| L3 | A51 | T1 | 151 | 27 | 20 | 176 | 34 | 34 | 442 | LH only |
| L4 | A60 | T1 | 72 | 22 | 23 | 94 | 24 | 27 | 262 | LH only |
| M1 | D06 | T4 | 617 | 60 | 77 | 714 | 97 | 106 | 1671 | wide |
| M2 | C73 | T3c | 143 | 18 | 20 | 181 | 28 | 18 | 408 | LH only |
| M3 | D02 | T4 | 220 | 22 | 28 | 293 | 38 | 60 | 661 | wide |
| M4 | D08 | T4 | 284 | 53 | 37 | 332 | 46 | 42 | 794 | wide |

5 Discussion

5.1 PNs innervating T4 cluster glomeruli

Three projection neurons running within the m-ACT and sending their dendrites to glomeruli of the T4 cluster were stained. These neurons exhibit a morphology that differs from other olfactory uniglomerular PNs of either the m- or l-ACT. Distinct features are: broad innervations of LPL that extend the borders of the LH, short branches projecting towards the PCT in the dorsal protocerebral lobe with boutons formed in its close proximity, a higher number of ascending collaterals from the IRT towards the MB's lips and a much higher amount of boutons, compared to other ACT PNs stained here and compared to data from other studies (Abel et al., 2001; Müller et al., 2002).

It was shown that these three neurons have their somata located in the medial, ventral rim of the antennal lobe (Fig. 4) in a position different from the location of the mSC2 soma cluster described by Kirschner et al. (2006), which leads to the assumption that there might be a fourth cluster of m-ACT PN somata which consists of T4 glomeruli innervating PNs exclusively.

The glomerulus D02 is innervated by one of these m-ACT neurons (Fig. 4E,

this study) which was not possible to show by several retrograde mass fillings of Kirschner et al. (2006) which may be due to different dextran-dye transporting properties of the cell. In this study a very small molecule, NeurobiotinTM, was used and the cells were filled anterogradely.

One m-ACT neuron, M2, exhibits the classical olfactory PN morphology with arborizations in the LPL restricted to the LH (Fig. 3 F). This neuron forms its dendritic field within a glomerulus that is lying between T3 glomeruli but was accounted to the T4 cluster and named D07 by Galizia et al. (1999a). However, Kirschner et al. (2006) assigned this glomerulus according to its position, morphology, innervation pattern and the fact that no branches of the T4 tract could be found to innervate it, to the T3c cluster and named it C73. The fact that this glomerulus does not belong to the T4 cluster can be supported by this study because the m-ACT neuron that was found to innervate this glomerulus (M2, figure 4 D) does not exhibit the special morphological features, found in the other T4 glomeruli innervating PNs, in this study.

Projection areas of these T4 m-ACT PNs within the LPL correspond to the broad band formed by the lateral bridge and the triangle (Kirschner et al., 2006). Projections of T4 m-ACT PNs extensively arborize and bear a high number of boutons in this region, hence they are likely to form output here. On the other hand the zone around the alpha lobe, the ring neuropil, is hardly innervated with only a few boutons found in close proximity to the alpha lobe/ pedunculus. Additionally, areas of the posterior LPL that might correspond to this region were described to get multimodal input by optical fibers and projections of the antennal tracts T6-1 and T6-3 (Maronde, 1991), and several classes of MB extrinsic neurons like A4 and A5 have also axonal endings here (Rybäk and Menzel, 1993). Thus, generally, the LPL gets multimodal inputs

of which this from the AL comes either direct via multiglomerular ml-ACT PNs, or indirect, conveyed to the MBs by uniglomerular PNs of the m- and l-ACT and from there via MB extrinsic neurons of several classes. Direct uniglomerular input to the LPL outside the LH seems to be restricted to the T4 m-ACT fibers shown here.

As it is not possible to apply genetic tools for the staining of PNs in the honeybee like it is in *Drosophila melanogaster* (Marin et al., 2002; Wong et al., 2002; Lin et al., 2007), reproducible staining of neurons that innervate the same glomerulus or staining even the same neuron multiple times, is very hard to achieve. Hence no statement of a stereotypic innervation of individual cells can be made. However, a distinct feature of PNs innervating the group of T4 glomeruli can be stated since the T4 cluster consists of only seven glomeruli of which three were stained here. One, D08, was previously described in Kirschner et al. (2006). They exhibit morphological features that differ from other PNs. In addition, a PN that innervates aT4 glomerulus in Abel et al. (2001, Fig. 5) sends off the same conspicuous branch from the dorsal protocerebral lobe like M3 in this study (Fig. 13 B) and glomerulus shape and soma position are also very similar (Fig. 4 E). However as only three individual neurons that have their dendrites in T4 glomeruli were stained, more data is needed to unerringly attribute the features found only to this group of PNs.

Possible roles of T4 glomeruli

Glomeruli of the T4 cluster have some features in common that separate them from the rest of the AL's glomeruli: they are all comparably large and when stained via the antennal tract they exhibit no layering in an innervated rim and a non innervated core region as other glomeruli do, instead they show a homogeneous innervation throughout the whole depth (Arnold et al., 1985; Kirschner et al., 2006). In the ALs of

the moth *Manduca sexta* PNs innervating the big pheromone sensitive macroglomerular complexes (PIa(MGC) fibers) were shown to have a similar morphology as the T4 m-ACT PNs described here. These neurons run via the inner ACT which is homologue to the m-ACT in *Apis mellifera*, innervate the MB calyces and then project to the posterior protocerebrum, but not to the LH where fibers that do not innervate MGC glomeruli project to (Homberg et al., 1988). However, the macroglomerular complexes (MGC) are male specific and hence do not exist in females like the honeybee workers studied here. But homologue structures exist in the ALs of drones of *Apis mellifera* here called macroglomeruli 1-4 (Arnold et al., 1985). A pheromonal subsystem within the antennal lobe of the females of social insects would make sense as lots of social communication takes place by the mean of pheromones. However, the T4 glomeruli appear not to be homologue to the macroglomeruli as they are existent in the drones AL too (Arnold et al., 1985) which does not exclude a possible role in a hypothetical social pheromone system. Brown et al. (2002) analyzed the ultrastructure of two glomeruli in *Apis mellifera* workers, A44 (T1 cluster) and D02 (T4 cluster) (a PN innervating D02 was stained here, preparation M3). Both glomeruli show an increase in volume when worker bees are in foraging age and leave the hive, this outgrowth is accompanied by an increase in the number of synapses in the A44 but not in the D02 glomerulus (Brown et al., 2002). The authors suggest that most of the synaptic connections within this glomerulus are already made before adult emergence and hence it may play a role in tasks that are relevant for a honeybee worker from the beginning of its adult live, such as social interactions that take place via tactile or chemosensory cues. The detection of pheromones relevant for social communication would fit into this suggestions, as well as a bilateral T4 innervating AL neuron, responding to antennal contact with bees wax only, that was described by Abel et al. (2001).

As m-ACT neurons that innervate T4 glomeruli express a very high number of boutons across the whole MB lip, this might indicate a diverging of the conveyed information onto many Kenyon cells and thus could be seen as very strong input. In combination with the boutons in close proximity to the PCT, which putatively could synapse onto axons of the GABAergic feedback neurons that run in this tract (Grünewald, 1999) and synapse onto extrinsic and intrinsic cells within the lip (Ganeshina and Menzel, 2001; spiny extensions of boutons in this study), other olfactory input could be suppressed and therefore T4 m-ACT PNs input emphasized.

5.2 Projections of m- and l-ACT PNs

A digital tool to analyze the distribution of cellular substructures within a neuropil was evolved and used on presynaptic boutons of PNs within the MBs lip. One advantage of this kind of analysis is that single cell preparations become comparable across individuals by dividing a neuropil in defined zones or calculating relative distances between a neuropils centerline and surface. Possible failures during the procedure might arise through the dependence on the manual abilities and the experience of the person who is reconstructing the neuron (SkeletonTree) and neuropil (labelfield) as these are still semi-automatic processes. The staining protocol is another aspect that might increase variability in the reconstructions as some possible zones are visible with one technique but not the other as seen here for the distal collar zone (Fig. 8 D). These tools (see 3.6.3 and 3.6.4) might also be suitable to compare the morphological data of a single neuron before and after registration into a common framework, like the honeybee standard atlas (Brandt et al., 2005), and hence offer a way to measure

a possible aberration of a neurons position (with respect to its course in the original preparation) within a neuropil during this registration process.

Mushroom body lip

L-ACT PNs show homogeneous bouton density in the lips, with a pattern that does not differ between anterior and posterior parts or the medial and lateral lip. This is not true for two l-ACT neurons shown in Abel et al. (2001) that have different patterns across lips and in anterior and posterior direction. The innervation pattern observed by Kirschner et al. (2006) in mass stainings indicates that l-ACT neurons innervate the lip homogeneously but omit a layer next to the surface of the outer lip, which would indicate a higher amount of boutons to be found in the inner lip when applying the four zones of figure 10. This is only the case for one preparation (Fig. 10 C), the opposite is found in the other three. Figure 8 B additionally shows a l-ACT branch that projects into the outer lip region. Thus, l-ACTs are present across all lip regions defined here but single cells innervate inner and outer lip heterogeneously. Bouton distribution with respect to the relative distance from the centerline also showed heterogeneous patterns with neurons exhibiting clear peaks or neurons having boutons equally distributed. Interestingly the patterns in corresponding lips of each individual neuron are rather similar. However, no common principles in bouton distribution for either m- and l-ACT PNs could be observed regarding the relative distance from the centerline and a restriction of l-ACT PN innervation to the lips central core as observed by Krofczik (2006) can not be accounted to the stained l-ACT neurons in this study. All neurons seem to have relative few boutons in the region next to the centerline but this might be due to the definition of bins around the centerline and the thus rising bin surface towards the lip periphery. On the other

hand minima can be observed in the bin next to the surface too.

Analysis of m-ACT PNs revealed more heterogeneous bouton density patterns between preparations, between lips of a single preparation and even within a single lip. This heterogeneity is also found for LH innervations and the overall number of boutons within this group. Different patterns of bouton distribution can also be seen in four preparations in Abel et al. (2001) and varying bouton density along the lip was also suggested by Krofczik (2006).

The clear segregation of m- and l-ACT input within the lip that was described by Kirschner et al. (2006) could not be found on a single cell level. This does not necessarily disprove Kirschner et al.'s results by several reasons. The number of neurons stained here represents around 1 % of all PNs running in both tracts (Rybäk, 1994), single cells variation in their branching might as well contribute to a common scheme seen in mass fills, and most of the m-ACTs stained here belong to a distinct subgroup that originates from the small cluster of seven T4 glomeruli and exhibit a different morphology compared to the majority of m-ACT PNs.

Distal collar

ACT PNs could be shown to express *en passant* blebs in a distal collar zone that was previously described (Gronenberg, 2001; Strausfeld, 2002) and shown to get optical (Ehmer and Gronenberg, 2002) as well as gustatory input (Schröter and Menzel, 2003). As olfactory input is conveyed to this zone too (this study) it must be considered as a multimodal input site like the BR.

Lateral horn

The LH innervations of l- and m-ACT PNs was found to resample the zones described by Kirschner et al. (2006) when excluding the three m-ACT PNs that innervate T4 glomeruli. Each of these three neurons exhibited a completely different branching pattern in this region, ranging from overall to very sparse innervation.

Possible connections

Kenyon cells of type I have large parts of their dendritic fields overlapping with their neighbors and neighboring Kenyon cells of the same morphological class bundle their axons, sending them as discrete bundles towards the lobes (Mobbs, 1982). The domain-like innervation of the lips by ACTs found here could indicate a separation of olfactory cues onto specialized Kenyon cell domains around the lip.

As previously discussed by Kirschner et al. (2006) the lip zones analyzed here (an inner and an outer lip) fit pretty well to the different dendritic field morphologies of spiny type I Kenyon cells described by Strausfeld (2002). These dendritic fields extend either over the whole cross section of the lip or are restricted to either the inner or outer half, expressing spines and thus might form input synapses with the presynaptic boutons of PNs in this region. Results from this study approve the subdivision of the lip into different innervated zones but also show that single l-ACT PNs projections to the lip are less stereotyped as previous mass stainings would let conclude, and that lip regions one tract as whole seems to omit (outer lip in Kirschner et al. 2006) are indeed innervated by single cells. Single l-ACT projections in a peripheral part of the lip that was supposed to be innervated by m-ACT PNs solely might synapse to type I and II Kenyon cells that extend their dendrites the

whole depth of the lip, but they also might connect to the spiny type I Kenyon cells that have their dendrites only in the outer lip. Thus this type of Kenyon cells would not convey only tract specific information as supposed. Another finding in favor for not only multi tract, but even for multi modal integration is the fact that m- and l-ACT PNs bear *en passant* blebs in the distal collar region. Not only that both tracts run here in close proximity but this region gets input from multiple sensory modalities including optical and gustatory information (Ehmer and Gronenberg, 2002; Schröter and Menzel, 2003). Strausfeld (2002) shows type I and II Kenyon cells that express spines or claws in the distal collar region. Also one spiny type I cell that innervates the inner part of both, distal collar and lip (Strausfeld, 2002, figure 2 E). Thus, multimodal input to the distal collar might be conveyed to the lobes by either type I or type II Kenyon cells and a special group of type I cells might also combine olfactory input to the lip with multimodal from the distal collar. The converging input of different kinds also makes this part of the collar suitable as a putative site for coincidence detection. Not only that the inner and outer lip and the distal collar are differentially innervated by several input neurons and Kenyon cells, Bartels (2007) could show segregated input of A3 feedback neurons to the outer lip and the distal collar.

5.3 Outlook

A 3D analysis of more PNs is needed, especially of m-ACTs that do not innervate T4 glomeruli of. Already existing data, either single cell scans or already reconstructed PNs could be easily extended by bouton data and feed into a database. The lip should be dissected into more than the four zones shown here in order to get more

precise results, for example a medial zone could be added and analysis of the zones could be combined with the data from the distance measurements. Zone orientated analysis could also be extended to other parts of the MBs or the LH. The same analysis should also be done on neurons that have been registered into the honeybee standard brain and compared to the non registered data. For further analysis of the domain-like innervation of the lip by all stained neurons but the T4 m-ACT, these lip domains should be compared between PNs of both tracts and PNs responding to the same odors by using the honeybee standard atlas (Brandt et al., 2005). Distal collar input of different modalities should be mapped to this region and possible overlapping analyzed, again by using the honeybee standard atlas. More data of T4 m-ACT PNs, physiological and morphological, is needed in order to reveal a possible involvement in the processing of sensory cues other than olfaction. Vibratome slices of given whole mount preparations would help to scan LPL projections with a higher resolution and allow a 3D reconstruction of branches in this part of the brain.

Bibliography

- Abel, R., Rybak, J., and Menzel, R. (2001). Structure and response patterns of olfactory interneurons in the honeybee, *apis mellifera*. *J Comp Neurol*, 437(3):363–383.
- Arenas, A., Fernández, V. M., and Farina, W. M. (2007). Floral odor learning within the hive affects honeybees' foraging decisions. *Naturwissenschaften*, 94(3):218–222.
- Arnold, G., Masson, C., and Budharugsa, S. (1985). Comparative study of the antennal lobes and their afferent pathway in the worker bee and the drone (*apis mellifera*). *Cell Tissue Res*, 242:593–605.
- Bartels, R. (2007). Ionenströme und Morphologie von GABA-immunoreaktiven Neuronen (A3) der Pilzkörper von *Apis mellifera* L. Master's thesis, Freie Universität Berlin.
- Bicker, G. (1999). Histochemistry of classical neurotransmitters in antennal lobes and mushroom bodies of the honeybee. *Microsc Res Tech*, 45(3):174–183.
- Bicker, G., Kreissl, S., and Hofbauer, A. (1993). Monoclonal antibody labels olfactory and visual pathways in drosophila and *apis* brains. *J Comp Neurol*, 335(3):413–424.
- Bicker, G., Schäfer, S., and Kingan, T. G. (1985). Mushroom body feedback interneurons in the honeybee show gaba-like immunoreactivity. *Brain Res*, 360(1-2):394–397.
- Bittermann, M. E., R., M., and Andrea Fietz, S. S. (1983). Classical conditioning of proboscis extension in honeybees (*apis mellifera*). *J Comp Psych*, 97:107–119.
- Brandt, R., Rohlfing, T., Rybak, J., Krofczik, S., Maye, A., Westerhoff, M., Hege, H.-C., and Menzel, R. (2005). Three-dimensional average-shape atlas of the honeybee brain and its applications. *J Comp Neurol*, 492(1):1–19.
- Brown, S. M., Napper, R. M., Thompson, C. M., and Mercer, A. R. (2002). Stereological analysis reveals striking differences in the structural plasticity of two readily identifiable glomeruli in the antennal lobes of the adult worker honeybee. *J Neurosci*, 22(19):8514–8522.

- Ehmer, B. and Gronenberg, W. (2002). Segregation of visual input to the mushroom bodies in the honeybee (*apis mellifera*). *J Comp Neurol*, 451(4):362–373. mb, optic.
- Erber, J., Masuhr, T., and Menzel, R. (1980). Localization of short-term memory in the brain of the bee, *apis mellifera*. *Physiological Entomology*, 5:343–358.
- Esslen, J. and Kaissling, K.-E. (1976). Zahl und Verteilung antennaler Sensillen bei der Honigbiene (*Apis mellifera L.*). *Zoomorphologie*, 83:227–251.
- Evers, J. F., Schmitt, S., Sibila, M., and Duch, C. (2005). Progress in functional neuroanatomy: precise automatic geometric reconstruction of neuronal morphology from confocal image stacks. *J Neurophysiol*, 93(4):2331–2342.
- Fahrbach, S. E. (2006). Structure of the mushroom bodies of the insect brain. *Annu Rev Entomol*, 51:209–232.
- Farina, W., Grüter, C., Acosta, L., and Cabe, S. M. (2007). Honeybees learn floral odors while receiving nectar from foragers within the hive. *Naturwissenschaften*, 94(1):55–60.
- Flanagan, D. and Mercer, A. R. (1989). An atlas and 3-d reconstruction of the antennal lobes in the worker honey bee, *apis mellifera* l. (hymnoptera: Apidae). *J Insect Morphol Embryol*, 18:145–159.
- Galizia, C. G., McIlwrath, S. L., and Menzel, R. (1999a). A digital three-dimensional atlas of the honeybee antennal lobe based on optical sections acquired by confocal microscopy. *Cell Tissue Res*, 295(3):383–394.
- Galizia, C. G., Sachse, S., Rappert, A., and Menzel, R. (1999b). The glomerular code for odor representation is species specific in the honeybee *apis mellifera*. *Nat Neurosci*, 2(5):473–478.
- Ganeshina, O. and Menzel, R. (2001). Gaba-immunoreactive neurons in the mushroom bodies of the honeybee: an electron microscopic study. *J Comp Neurol*, 437(3):335–349.
- Grünwald, B. (1999). Morphology of feedback neurons in the mushroom body of the honeybee, *apis mellifera*. *J Comp Neurol*, 404(1):114–126.
- Gronenberg, W. (2001). Subdivisions of hymenopteran mushroom body calyces by their afferent supply. *J Comp Neurol*, 435(4):474–489.
- Hammer, M. (1993). An identified neuron mediates the unconditioned stimulus in associative olfactory learning in honeybees. *Nature*, 366:59–63.

- Hammer, M. (1997). The neural basis of associative reward learning in honeybees. *Trends Neurosci*, 20(6):245–252.
- Hammer, M. and Menzel, R. (1998). Multiple sites of associative odor learning as revealed by local brain microinjections of octopamine in honeybees. *Learn Mem*, 5(1-2):146–156.
- Hildebrand, J. G. and Shepherd, G. M. (1997). Mechanisms of olfactory discrimination: converging evidence for common principles across phyla. *Annu Rev Neurosci*, 20:595–631.
- Homberg, U., Montague, R. A., and Hildebrand, J. G. (1988). Anatomy of antennocerebral pathways in the brain of the sphinx moth *manduca sexta*. *Cell Tissue Res*, 254(2):255–281.
- Howse, P. E. (1974). *Experimental analysis of insect behaviour*, chapter Design and function in the insect brain, pages 180–194. Springer, Berlin, Germany.
- Kelber, C., Rössler, W., and Kleineidam, C. J. (2006). Multiple olfactory receptor neurons and their axonal projections in the antennal lobe of the honeybee *apis mellifera*. *J Comp Neurol*, 496(3):395–405.
- Kenyon, F. (1896). The brain of the bee. a preliminary contribution to the morphology of the nervous system of the arthropoda. *J Comp Neurol*, 6:134–210.
- Kirschner, S., Kleineidam, C. J., Zube, C., Rybak, J., Grünwald, B., and Rössler, W. (2006). Dual olfactory pathway in the honeybee, *apis mellifera*. *J Comp Neurol*, 499(6):933–952.
- Krofczik, S. (2006). *The Honeybee Olfactory System: 3-D Anatomy, Physiology and Plasticity*. PhD thesis, Freie Universität Berlin.
- Kuwabara, M. (1957). Bildung des bedingten Reflexes von Pavlovs Typus bei der Honigbiene, *Apis mellifica*. *J Fac Hokkaido Univ Ser VI Zool*, 13:458–464.
- Lin, H.-H., Lai, J. S.-Y., Chin, A.-L., Chen, Y.-C., and Chiang, A.-S. (2007). A map of olfactory representation in the drosophila mushroom body. *Cell*, 128(6):1205–1217.
- Marin, E. C., Jefferis, G. S. X. E., Komiyama, T., Zhu, H., and Luo, L. (2002). Representation of the glomerular olfactory map in the drosophila brain. *Cell*, 109(2):243–255.
- Maronde, U. (1991). Common projection areas of antennal and visual pathways in the honeybee brain, *apis mellifera*. *J Comp Neurol*, 309(3):328–340.

- Menzel, R. (2001). Searching for the memory trace in a mini-brain, the honeybee. *Learn Mem*, 8(2):53–62.
- Menzel, R. and Giurfa, M. (2001). Cognitive architecture of a mini-brain: the honeybee. *Trends Cogn Sci*, 5(2):62–71.
- Menzel, R. and Giurfa, M. (2006). Dimensions of cognition in an insect, the honeybee. *Behav Cogn Neurosci Rev*, 5(1):24–40.
- Müller, D., Abel, R., Brandt, R., Zöckler, M., and Menzel, R. (2002). Differential parallel processing of olfactory information in the honeybee, apis mellifera l. *J Comp Physiol A Neuroethol Sens Neural Behav Physiol*, 188(5):359–370.
- Mobbs, P. G. (1982). The brain of the honeybee apis mellifera. i. the connections and spatial organization of the mushroom bodies. *Phil. Trans. R. Soc. Lond. B*, 298:309–354.
- Rybak, J. (1994). *Die strukturelle Organisation der Pilzkörper und synaptische Konnektivität protocerebraler Interneuronen im Gehirn der Honigbiene, Apis mellifera*. PhD thesis, Freie Universität Berlin.
- Rybak, J. and Menzel, R. (1993). Anatomy of the mushroom bodies in the honey bee brain: the neuronal connections of the alpha-lobe. *J Comp Neurol*, 334(3):444–465.
- Sachse, S. and Galizia, C. G. (2003). The coding of odour-intensity in the honeybee antennal lobe: local computation optimizes odour representation. *Eur J Neurosci*, 18(8):2119–2132.
- Schmitt, S., Evers, J. F., Duch, C., Scholz, M., and Obermayer, K. (2004). New methods for the computer-assisted 3-d reconstruction of neurons from confocal image stacks. *Neuroimage*, 23(4):1283–1298.
- Schürmann, F. W. (1974). Bemerkungen zur Funktion der Corpora pedunculata im Gehirn der Insekten aus morphologischer Sicht. *Exp. Brain Res.*, 19:406–432.
- Schröter, U. and Menzel, R. (2003). A new ascending sensory tract to the calyces of the honeybee mushroom body, the subesophageal-calycal tract. *J Comp Neurol*, 465(2):168–178.
- Strausfeld, N. J. (2002). Organization of the honey bee mushroom body: representation of the calyx within the vertical and gamma lobes. *J Comp Neurol*, 450(1):4–33.
- Suzuki, H. (1975). Antennal movements induced by odour and central projection of the antennal neuron in the honeybee. *J. Insect Physiol.*, 21:831–847.

- Takeda, K. (1967). Classical conditioned response in the honey bee. *J Comp Neurol*, 6:168–179.
- von Frisch, K. (1967). *The dance language and orientation of bees*. Harvard University Press, Cambridge, MA.
- Witthöft, W. (1967). Absolute Anzahl und Verteilung der Zellen im Hirn der Honigbiene. *Zoomorphology*, 61(1):160–184.
- Wong, A. M., Wang, J. W., and Axel, R. (2002). Spatial representation of the glomerular map in the drosophila protocerebrum. *Cell*, 109(2):229–241.

Danksagung

Zuerst möchte ich Professor Menzel dafür danken, dass diese Diplomarbeit betreut hat und mir ermöglicht hat diese in seiner Arbeitsgruppe anzufertigen.

Dr. Sabine Krofczik danke ich dafür, dass sie mich für das Thema dieser Arbeit begeistert hat, welches aus Ihrer Dissertation hervorgegangen ist.

Mein ganz besonderer Dank gilt Anja Kuss vom Zuse Institut, die zusammen mit mir die Tools zur Auswertung der 3D Daten erarbeitet und auch spontane Ideen noch kurzfristig umgesetzt und für mich programmiert hat.

Dr. Jürgen Rybak bin ich überaus dankbar dafür, dass er immer ein offenes Ohr für die vielen Fragen und Diskussionen zu anatomischen und auch methodischen Themen hatte.

Astrid Klawitter und Gisela Manz danke ich sehr für die große Unterstützung in labortechnischen Fragen und die Bereitstellung der Chemikalien und Lösungen.

Für die gute Zeit im Labor, auch während technischer Ausfälle von konfokalem Mikroskop und Laserpuller danke ich meiner "Leidensgenossin" Ruth Bartels.

Außerdem danke ich allen Mitgliedern der AG Menzel und der AG Pflüger dafür, dass ich mich in allen Fragen stets an sie wenden konnte und für die zwar anstrengenden aber dennoch wunderbaren letzten Monate.

Meinen Freunden und Verwandten möchte ich für ihre Aufmerksamkeit und Auffmunterungen vor allem in der anstrengenden letzten Phase dieser Arbeit danken.

Der größte Dank jedoch gilt meinen Eltern, die mir mein Biologie Studium ermöglicht und mich auf dem Weg hierher stets unterstützt haben, und meiner Freundin Ina Pietruschke die gerade in den letzten Wochen ein ungeheures Verständnis aufgebracht und mir immer wieder Kraft gegeben hat.